ANATOMY OF A CORTICAL-STRIATAL-THALAMIC NETWORK MEDIATING DIRECTED ATTENTION IN THE RAT

By

JOSEPH LATON CHEATWOOD

A DISSERTATION PRESENTED TO THE GRADUATE SCHOOL
OF THE UNIVERSITY OF FLORIDA IN PARTIAL FULFILLMENT
OF THE REQUIREMENTS FOR THE DEGREE OF
DOCTOR OF PHILOSOPHY

UNIVERSITY OF FLORIDA

2004

For the great neuroscientists, men and women, who have gone before, and those who will come. Giants, thank you for lending your shoulders, on which I stand.

I now offer mine.

ACKNOWLEDGMENTS

I thank the innumerable people who have contributed to my making it to this point in life. I thank my folks and sisters for bringing me up as best they could and giving me a head start in life. I thank Nancy Smith, my AP Biology teacher at Lake Gibson High School in Lakeland, Florida. Under her guidance, I saw how little of the natural world we understand. I thank the great professors at Stetson University, especially Peter May and Terence Farrell, for encouraging my interest in the sciences and being great friends. I couldn't have done all of the processing without Maggie Stoll. Tanya McGraw-Ferguson showed me the wonder of teaching, and the value of strength. Diana Sarko sat next to me for the last year or two, and I do not know how I would have made it without her as my cheering section. I thank all of the members of my committee for giving of their time to oversee my work. Jim Corwin has always been able to make me think and, above all, laugh aloud despite myself. He also gave me several pieces of sound advice that changed my life in many ways. I appreciate it, no matter how many ivy-leaguers laugh in my face. Above all, I thank Roger Reep for being an excellent mentor. His support has helped me get through the tough times, which unavoidably accompany life.

TABLE OF CONTENTS

Page

LIST OF FIGURES

Abstract of Dissertation Presented to the Graduate School
of the University of Florida in Partial Fulfillment of the
Requirements for the Degree of Doctor of Philosophy

ANATOMY OF A CORTICAL-STRIATAL-THALAMIC NETWORK MEDIATING DIRECTED ATTENTION IN THE RAT

By

Joseph Laton Cheatwood

August 2004

Chair: Roger L. Reep
Major Department: Veterinary Medicine

The anatomy of a cortical-subcortical network mediating directed attention in the rat was investigated via retrograde, single anterograde, and multiple anterograde labeling. The rat dorsocentral striatum (DCS) is essential for the proper functioning of the directed attention network. Region DCS is defined as the central terminal field for corticostriatal axons originating in medial agranular cortex (AGm). Cortical and thalamic afferents to DCS were first defined by placing a retrograde tracer in DCS, and observing the resultant pattern of cortical and thalamic labeling. In this way, it was determined that the cortical areas AGm, PPC, VLO, and Oc2M project most consistently to DCS. Thalamic regions LP, LD, MD, and VL were labeled selectively, depending on the placement of the retrograde tracer in DCS. Anterograde tracing experiments were performed to further explore the pattern of labeling observed in the retrograde study. Multiple injections of fluorescent anterograde tracers were used to visualize the patterns of overlap and interdigitation of cortical and thalamic regions with cortical area AGm. Cortical areas

PPC and Oc2M were found to form dense foci of axonal terminals in DCS. These foci are regions of intense overlap with axons from area AGm, and may represent important regions of convergence on striatal medium spiny neurons. Lastly, a novel model of focal photothrombosis was developed in an effort to maximize the physiological similarities of the rat neglect model and human neglect, which is most frequently caused by a stroke affecting the middle cerebral artery.

CHAPTER 1
INTRODUCTION

Over the last 20 years, several areas of research have focused on basal ganglia diseases and disorders with the goal of understanding the pathophysiology, and the development of therapeutic agents. In humans, diseases of the basal ganglia are most commonly associated with movement disorders, either hypokinetic (Parkinson's disease), or hyperkinetic (Huntington's disease) [20]. One broad clinical goal is the successful development of new, more beneficial treatments and management strategies for disorders of cortico-basal ganglia-thalamo-cortical loops subtending motion, directed attention, and other brain functions. To create therapies for complex central nervous system (CNS) disorders, we need a better understanding of the role of the basal ganglia in functional CNS loops. This discussion considers what is currently known about the anatomy and function of these circuits, with a specific focus on striatal projections from cortical and thalamic neurons.

Striatal Anatomy and Topography

The basal ganglia are a collection of nuclei located in the forebrain and midbrain of most vertebrate species. These nuclei are known to play a role in movement, attention, and cognition; but their functions are not fully understood. The basal ganglia are composed of the caudate nucleus, putamen, globus pallidus, substantia nigra, and the subthalamic nucleus of the thalamus, which are all interconnected. The neostriatum is a subset of the basal ganglia, and is composed of the caudate nucleus, the putamen, and the nucleus accumbens. The nuclei of the neostriatum are discrete in primates, but are fused

in rodents [133]. For this reason, the rat neostriatum is also synonymously referred to as the caudato-putamen [76]. There are several types of neurons in the striatum, but the subtype receiving the most attention is the medium spiny neuron.

Efferent projections from cortical areas or thalamic nuclei enter the basal ganglia in several places, and form synapses on medium spiny neurons in the caudate nucleus and putamen [40,85,133]. The neostriatum receives convergent inputs via afferent fibers from sensory, motor, and associational cortical areas; the intralaminar nuclei of the thalamus; substantia nigra pars compacta (SNc); and the dorsal raphé nucleus. Most of these inputs are glutamatergic, with the exception of those from SNc and the dorsal raphé nucleus, which are dopaminergic and serotoninergic, respectively [40,85,133]. The densest projections to the neostriatum come from the cortex and the intralaminar nucleus of the thalamus. Most synapses (85%) on the primary neurons of the striatum (medium spiny neurons) are formed by axonal projections from these two contributors [55,66]. This strong interrelation suggests an important integrative role of cortical and thalamic connections to striatal neurons.

Anatomical evidence suggests that the striatum may play an important role in the integration of information coming from multiple cortical areas and thalamic nuclei. Axons from cortical and thalamic neurons arborize in the striatum in a morphology termed “cruciform axodendritic” by Ramón y Cajal, in reference to the relatively straight course the axons follow, forming synapses with dendrites of medium spiny neurons as they pass [90]. These axons have been shown to enter the striatum and travel long distances along the rostrocaudal plane, synapsing all along their length with numerous striatal neurons [54].

Interestingly, individual striatal neurons receive relatively few synapses from a given axon as a result of the cruciform axodendritic morphology of cortical afferents [108]. Considering this fact in concert with the prevalence of cortical synapses on medium spiny neurons (80%, as previously noted), individual medium spiny neurons likely receive input from multiple cortical areas [133]. Similarly, the small number of striatal cells available to receive input relative to the number of cortical cells projecting to the striatum has led many to hypothesize that the striatum is a site of convergence for information from multiple brain regions [17,85,133].

Cortical inputs to the striatum have been studied in some detail, but data on the afferent projections of discrete cortical areas are incomplete, as are the data concerning the fine topography with which cortical areas project to the striatum. Anatomical and electrophysiological studies of corticostriatal connections date back to the 1800s. The first confirmation of the existence of corticostriatal projections came in the mid-1900s. In 1944, Glees provided the first unequivocal evidence of the existence of corticostriatal projections. Glees [42] used a recently developed silver-stain method to visualize the paths of degenerating axons after the destruction of selected cortical areas, and found that fibers do indeed project from the cortex to the striatum of the cat, contrary to many prior reports.

Since publication of Glees' paper report in 1944, several generations of axonal tracing methods (including autoradiography, horseradish-peroxidase, biotinylated dextran-amines, and a variety of anterograde and retrograde fluorescent tracers) have been used to expand on Glees' findings [99]. It is now accepted that all functional areas of the cerebral cortex send projections to some portion of the striatum. This has been

confirmed via retrograde and anterograde tract tracing in cat, rat, and primate models [4,36,50,75,76,91-93,98,99,106,131,134].

In addition to documenting which cortical areas send axonal projections to the striatum, important patterns related to the topography of these projections have been described. Kemp and Powell [56] first noted that axonal projections from individual cortical areas project to discrete and consistent striatal regions that follow the overall shape of the external capsule, with little overlap between areas. This pattern has been observed for many cortical areas [10,75,76,92]. In an expansion of this finding, Brown *et al*. [10] and Wright *et al.* [134] presented data supporting this pattern, but also noted that two areas of axon terminals can be seen after closely spaced injections in rat somatosensory cortex: one area of similar shape to that previously reported, and an additional area located medially in the striatum. Wright *et al.* [134] suggest that this pattern indicates the presence of at least two systems of corticostriatal projections terminating in the rat striatum, termed the “discrete” and “diffuse” systems.

The medial area of the striatum discussed by Brown *et al.* and Wright *et al*., among others, is the current focus of a rat model of hemispatial neglect [15,16,18,58,63,64,91-93,116]. This model focuses on a ~1 mm diameter portion of the rat striatum, located dorsomedially and extending throughout the rostrocaudal extent of the striatum, as a potential focal point for convergence of information coming from the medial agranular cortex (AGm) and the posterior parietal cortex (PPC), among other cortical areas. Focal injections of a retrograde tracer into this striatal area, referred to as the dorsocentral striatum (DCS), produce labeled cells in many cortical areas, depending on the precise

location of the injection, but most often in AGm, PPC, and orbital cortex (Chapter 2). Functional aspects of this model are discussed next.

In addition to the presence of unique mediolaterally and dorsoventrally discrete projections from cortical areas, these terminal fields are known to extend great distances in the rostrocaudal dimension [44,91-93,104,114]. In one seminal paper, Selemon and Goldman-Rakic [104] demonstrated that some cortical areas project axons that traverse the rostrocaudal extent of the primate caudate nucleus. In the same paper, Selemon and Goldman-Rakic demonstrated conclusively that projections arising from cortical areas: 1) terminate closely to one another in the striatum, 2) do not limit their projections to proximal portions of the striatum, and 3) partially overlap and interdigitate in the striatum. Taken together, these findings indicate that axons arising from individual cortical areas project to portions of the striatum in a consistent, partially overlapping, and partially interdigitating fashion, without regard to their initial anatomical proximity to one another.

Axons terminating in a given striatal territory can arise from either ipsilateral or contralateral cortical areas. Studies using several techniques arrived at this conclusion. Electrophysiological recordings from single striatal neurons responding to stimulation in both ipsilateral and contralateral cortical areas [130] and retrograde or anterograde tract tracing [75,76,92] have conclusively demonstrated the presence contralateral and ipsilateral axons sending projections to the striatum. These findings indicate that axons from both adjacent and distant ipsilateral cortical areas converge on single striatal neurons; and that convergence of information from homotopic contralateral cortical areas

also occurs in the striatum. These contralateral connections may allow for some interhemispheric synchronization of striatal activity [75,76].

Two broad methods are used to study corticostriatal projections via anterograde or retrograde tracers: studies of populations of neurons [10,93] or single-cell studies [89,101,135]. Each type of study is useful for answering different types of questions about corticostriatal projections, and both have advantages and disadvantages.

Studies of populations of axons allow for comparisons to be made between the projections of functional cortical areas, like AGm and PPC [93]. Additionally, these studies are useful in determining which cortical layers are involved in connections between two territories [39]. These studies can be difficult to interpret, however, if injections of anterograde tracers cross cytoarchitectural boundaries (i.e., injection on border of AGm and forelimb cortex). This potential problem with anterograde studies mandates that any findings from such studies be confirmed via retrograde injections directed at targets identified by anterograde methods [93].

Single-cell studies provide the relative advantage of being able to follow a single axon from its origin to its termination; noting its path, and noting whether any collateral projections stem from single axons of interest [89]. These studies are performed by inserting a pipette into individual neurons of interest, or placing a minute quantity of a tracer near a neuron, hopefully staining only one cell or very few cells [85]. Because of the impracticality of doing a large number of single-cell injections to determine all of the targets of a given cell population, studies of single neurons do not easily provide enough information about relative numbers of neurons projecting among areas of interest. Given

these benefits and pitfalls, single-neuron studies are excellent for examining the results of broader tracing studies, in much more detail.

By using single-neuron studies in the above fashion, researchers are able to more clearly define the way in which axonal arborizations of corticostriatal neurons relate to dendritic arborizations of striatal neurons. The original single-neuron studies were conducted by Ramón y Cajal, who examined Golgi-stained sections and described the structure of axons in the striatum, which he correctly surmised to be corticostriatal neurons [90].

In 1987, Wilson [131] published an important study using several different methods to look at individual cortical neurons and their efferent projections. In this study, Wilson used his data in addition to previous findings, to describe three different subpopulations of neurons projecting from cortical area AGm:

- A population located in layer V which projects to the brainstem. These cells also send collateral projections to ipsilateral striatum and at least some of their axons enter the pyramidal tract [67].
- A population of corticothalamic neurons in layer VI that send collaterals to striatum [100].
- A larger population of corticostriatal neurons in layer Va that do not project to the thalamus or brainstem. Single cells of this type form projections to contralateral cortex, ipsilateral striatum, and contralateral striatum [131].

As a result of his findings, Wilson speculates about the existence of neurons that are exclusively corticostriatal, stating that perhaps all of the corticostriatal afferents are collaterals of axons terminating elsewhere in the central nervous system [131].

Functional Implications of Anatomical Organization

The most basic functional unit of the striatum is the medium spiny neuron. These neurons make up the majority of cells in the striatum. Medium spiny neurons are the targets of afferent projections to the striatum, and are also the cells extending efferent projections out of the striatum [55]. Medium spiny neurons are considered to be tonically inactive, firing mainly in response to stimulation from cortical and thalamic inputs [17,132]. Since so many types of afferents contact medium spiny neurons, but so few synapses are contributed by any one afferent, the likelihood exists that striatal neurons may only fire in response to convergent stimulation from multiple afferent sources, indicating a potential role as an integrator of data from multiple cortical areas [133]. Cowan and Wilson provided preliminary support for this theory by demonstrating that the synchronization of multiple cells is needed for depolarization of medium spiny neurons [17]. The previously discussed interdigitation of cortical afferents allows the hypothesis that axonal inputs from multiple cortical regions firing together could stimulate striatal neurons. This hypothesis warrants further examination.

In addition to the convergence of cortical inputs, glutamatergic thalamic afferents, dopaminergic SNc projections, and serotoninergic projections from the dorsal raphé nuclei also contact single-medium spiny neurons in the striatum [9,69]. Dopamine also plays a role in the output of the striatum, via the differential expression of excitatory and inhibitory dopamine receptors (discussed is more detail below). Despite the lack of a clear model for the interaction of inputs using different neurotransmitters, one commonly accepted hypothesis is that dopaminergic inputs play a role in gating the output of striatal medium spiny neurons [41,83,86,106,124].

The striatum can be broken into functional subsystems with different projection patterns, neurological markers, neurotransmitter receptors, and end functions [40,78,79]. Gerfen refers to these pathways as the “striatonigral” and “striatopallidal” pathways, but they are most commonly known as the “direct” and “indirect” pathways, respectively [20]. Both the direct and indirect pathway share common endpoints: GPi and SNr. The direct pathway projects directly from the striatum to GPi and SNr, as the name suggests. The indirect pathway, however, projects first to GPe, then to the subthalamic nucleus, and finally to GPi and SNr.

The direct pathway encourages excitation of thalamic targets (positive feedback), while the indirect pathway exerts an inhibitory influence on excitatory thalamic projections, resulting in an overall inhibitory effect (negative feedback). Interestingly, medium spiny neurons respond differently to dopaminergic inputs from SNc to the striatum, depending on the pathway (direct or indirect) to which they project. This difference results from the selective expression of two types of dopamine receptors (called D1 and D2) on populations of medium spiny neurons. Striatal medium spiny neurons contributing to the direct pathway have D1 receptors, which are excitatory; and neurons contributing to the indirect pathway have D2 receptors, which are inhibitory [20].

The direct and indirect pathways were at one time broadly used to explain the function of striatal outputs to the basal ganglia. With today’s better understanding of striatal circuitry, the concept of the direct and indirect pathways is recognized as an oversimplified description of the role of the striatum in several currently hypothesized cortico-basal ganglia-thalamo-cortical loops.

The concept of multiple cortico-basal ganglia-thalamo-cortical loops was first popularized by Alexander *et al*. [1,2,85], who proposed the existence of five parallel loops involved in processing: motor, oculomotor, dorsolateral prefrontal, lateral orbitofrontal, and anterior cingulate circuits. Each of these loops uses a direct and an indirect pathway for striatal efferents [1].

The exact composition of cortico-basal ganglia-thalamo-cortical loops is currently unclear. Some have hypothesized that each parallel loop may be even further separated into subloops for more discrete functions, such as movement preparation and movement execution [1,79]. An alternate hypothesis to this parallel-loop concept is the existence of a "tripartite" striatum, with three functional and topographic subdivisions receiving inputs from closely functionally related cortical areas: the associative territory, the sensorimotor territory, and the limbic territory [84].

The two hypotheses are not entirely at odds, but the tripartite hypothesis places more emphasis on the integrative function of the striatum. A rat model of corticostriatal mechanisms for directed attention more closely resembles the patterns of connectivity predicted by Parént [84]. The previously mentioned rat model of hemispatial neglect is an example of a cortico-striatal network mediating an integrative function: directed attention. Experimental lesions of cortical area AGm, PPC, or striatal region DCS are sufficient to produce persistent multimodal neglect [15,16,58,63,64,91,97], as are lesions of axons connecting the areas [11].

In some animals with lesions in AGm or PPC, spontaneous recovery is possible [119]. Delivery of the dopamine agonist apomorphine either systemically or directly into DCS induces recovery of function after a lesion in either AGm or PPC [14,15,62], while

more lateral injections do not induce recovery [115,116,118]. In contrast to the cortical lesions, animals receiving excitotoxic axon-sparing lesions of DCS do not recover spontaneously, nor do they respond to apomorphine [115]. Therefore, behavioral and anatomical results from the neglect model support the conclusion that the DCS is a required element in a cortico-striatal circuit for directed attention.

In addition to the functional and topographic subdivisions previously discussed, the striatum can be further subdivided at the molecular level. Immunohistochemical staining of the calcium binding protein calbindin reveals an interesting mosaic pattern of staining in the rat striatum. The striatum contains opiate receptor-rich/calbindin-poor areas, called "patches," in a calbindin-rich/opiate receptor-poor sea, termed the "matrix" [38]. It has been hypothesized that this apparent compartmentalization may reflect the differential staining of functional units in the striatum [29,38].

Some debate exists, however, about the anatomical and functional importance of the patch and matrix compartments. Some of the literature supports the hypothesis that cortical areas project to both patch and matrix compartments in their corresponding striatal territories, but different areas predominantly project to one compartment or the other [39].

Gerfen [39,40] concluded that cortical projections to patch and matrix areas arise from different cortical layers: layer Vb and VI cortical neurons project principally to patches; while neurons in layers Va, II, and III project largely to the matrix. Gerfen also notes that neocortical areas project largely to the matrix, while allocortical areas send their projections to patches. Kincaid and Wilson confirmed these findings, adding that

there are probably multiple subtypes of corticostriatal neurons, each potentially finding different targets in the striatum [60].

Gerfen also hypothesizes that, in addition to receiving input from different cortical layers, patch and matrix compartments also differ in their efferent projections. He suggests that axons leaving patch compartments project largely to the dopaminergic substantia nigra pars compacta, and that axons from the matrix compartment project to the GABAergic neurons of the substantia nigra pars reticulata [37,38,40]. Despite Gerfen's data, no consensus on the functional importance of striatal patch and matrix compartments exists at this time. Specifically, the differential roles of patch and matrix compartments in cortico-basal ganglia-thalamo-cortical loops, if any, remain to be established.

Though striatal research has been conducted in rodents, cats, and primates, the majority of findings have been consistent. Obviously, some anatomical differences exist, especially between the rat and primate models. As previously mentioned, key differences exist in the basic arrangement of the basal ganglia in rats and primates. In primates and cats, the caudate and putamen are separate, non-overlapping structures and are separated from one another by the internal capsule. In rats, the two nuclei are blended together in the dorsal portion of the striatum, and the fibers that make up the internal capsule in cats and primates perforate the striatum in a much more diffuse arrangement.

In short, the anatomical and functional intricacies of the striatum, specifically regarding cortico-basal ganglia-thalamo-cortical loops, are not well understood. Future research on corticostriatal connections and loops should focus on issues such as

- Formation of synapses from functionally related cortical areas on individual corticostriatal axons

- The role of convergent stimuli from multiple inputs (cortical areas, thalamic inputs, etc.) in the generation of an action potentials by striatal neurons

- The definition of the functional subunits of the striatum and their relationship to cortical, thalamic, and brainstem afferents and efferents

- The development of clinical interventions to modify the function of cortico-basal ganglia-thalamo-cortical loops and generate functional recovery from lesions and diseases.

CHAPTER 2
CORTICAL AND THALAMIC PROJECTIONS TO THE DORSOCENTRAL STRIATUM IN RATS

Introduction

The dorsocentral striatum (DCS) is defined as the major site of termination of corticostriatal inputs originating from the medial agranular cortex (AGm or Fr2) in rats [6,30,93,94]. In the region of the striatum between the level of the genu and that of the anterior commissure (ac), DCS constitutes a territory ~1 mm in diameter, centered in the dorsal striatum ~0.5 to 1.5 mm below the external capsule, approximately equidistant from the medial and lateral boundaries of the striatum [93]. Area AGm is a multimodal association premotor cortex with diverse cortical connections [97], and DCS has been implicated as a multimodal convergence region of striatum [76,93].

As noted by Parent and Hazrati [85], once it became clear that the striatum has sensorimotor, associational, and limbic regions, it became important to determine the organizational subdivisions within these regions. Although association areas of the rat striatum have not been studied in the same detail as sensorimotor and limbic regions, several investigations have focused on striatal circuitry related to prefrontal cortical areas [7,8,46]. The study of association areas is of special interest because the influence of the striatum on motor function includes cognitive components [45] mediated by cortical areas like AGm. Thus, the associative striatum constitutes a substrate for the dynamic modulation of behaviors having a significant multimodal component involving association cortices.

The relationship between DCS and AGm is of particular interest, because each of these regions is a major component of the neuronal circuitry mediating directed attention. After the initial development of a rat model of hemispatial neglect [18,19], behavioral experiments identified AGm and the posterior parietal cortex (PPC) as being cortical areas critical for the normal functions of spatial orientation and directed attention [15,16,58,63,64]. In rats, lesions in either of these reciprocally interconnected [91,97] areas produce multimodal neglect, as does disconnection of their corticocortical connections without direct damage to AGm or PPC [11]. Spontaneous recovery from neglect resulting from cortical lesions occurs in some rats [119], and is correlated with reestablishment of symmetrical expression of immediate early genes and glutamate receptors in the dorsolateral striatum and DCS [120-122]. In addition, DCS is essential for spontaneous and pharmaceutical-induced recovery of function [115,116], and this points to the pivotal role of corticostriatal connections in directed attention.

Because of the critical role of DCS in the circuitry mediating directed attention and recovery from neglect, it is important to know which cortical areas are capable of influencing the activity of neurons in DCS. Thus, my study aimed to identify all the cortical inputs to DCS, and to interpret this pattern with regard to the known corticocortical connections of these areas. Specifically, because of the close anatomical and functional relationship between AGm and PPC, I wished to determine if cortical-area PPC projects to DCS. In addition, I wanted to determine if the thalamic nuclei that project to DCS include those that project to the cortical areas that provide input to DCS. For these purposes, I made injections of retrograde axonal tracers in DCS or along its margins. The results provide new information on corticostriatal and thalamostriatal

topography and convergence, support the behaviorally derived hypothesis that DCS functions as a striatal association area that is critical for directed attention, and provide a foundation for experiments intended to promote recovery from neglect, by therapeutic interventions.

Materials and Methods

Twenty-five male Long-Evans Hooded rats were anesthetized with an intraperitoneal injection of a ketamine/xylazine cocktail (90 mg/kg:10 mg/kg) and placed in a stereotaxic device. Either Fast Blue (Sigma, 3% in H_2O) or Diamidino Yellow (Sigma, 3% in H_2O), was injected into the striatum. Both are frequently used retrograde axonal tracers that produce reliable labeling with little spreading of the injection site relative to other tracers like Fluorogold [13]. Injections were made via Picospritzer (General Valve Corp., Fairfield, NJ) using 2 or 3 pulses of 20 to 30 psi, 5 to 20 msec duration; or via a 33 g Hamilton syringe using a volume of 0.05 to 0.10 μl. Some animals received a second injection of the other tracer in the opposite hemisphere, but this analysis involves only one tracer per animal. The injections in cases 93 and 94 were on the right side; all others were on the left. After a 3 to 5 day survival time, rats were injected IP with 3 mL chloropent (4.25% chloral hydrate, 0.9% pentobarbital) and perfused intracardially with 300 mL of potassium-buffered saline (PBS) followed by 300 mL of 4% buffered paraformaldehyde. Brains were then removed and stored in dilute fixative (0.4% paraformaldehyde), and cryoprotected by sinking in a 30% sucrose solution. Coronal sections were cut at 40 μm on a freezing microtome, and placed in dilute fixative until being mounted on slides. Three spaced series of sections were used

for analysis: one for viewing on a fluorescent microscope, a second for cresyl violet staining for cytoarchitectural analysis, and a third for fluorescent photomicrography.

Three-dimensional reconstructions of tracer-injection sites were produced by outlining areas of visible fluorescence and the boundaries of the striatum and cortex from fluorescent sections, transferring these sketches into vector drawings (Adobe Illustrator 10), then making three-dimensional models and rendering final images using an M5 imaging system (Imaging Research, Inc). Cases 93 and 94 are represented on the left for comparison purposes, even though their injections were located on the right side.

Thalamic and cortical labeling were evaluated using an Olympus BH-2 fluorescent-equipped microscope. Sections were examined at 20x primary magnification for labeled cells in any cortical areas or thalamic nuclei. The locations of labeled cells were determined by cytoarchitectural examination of adjacent cresyl-violet-stained sections, and with reference to the cytoarchitectural criteria of Zilles and Wree [137] for cerebral cortical areas. The terms AGm and AGl are synonymous with their areas Fr2 and Fr1, respectively. The terms rAGm and cAGm refer to the rostral and caudal subregions of AGm that are located rostral and caudal to the level of the genu, and have different patterns of functional representations [30,82] and anatomical connections [97]. Area PPC is located at approximately AP –3.4 to –4.4 mm relative to bregma, between ML 1.5 to 4.5mm [16,91]; and was distinguishable from the caudally adjacent area Oc2M by the appearance of layer V in Nissl stained sections, in most brains. In PPC, layer V merges with layer IV superficially and with layer VI basally. In area Oc2M, the boundaries of layer V with layers IV and VI are more distinct, because of reduced cell density in the superficial and basal portions of layer V. Thalamic nuclei were identified

and delineated according to the criteria and maps of Jones [53] and Paxinos and Watson [87]. Analysis of labeled cells was limited to the hemisphere ipsilateral to the tracer injection. Cases having injection sites that encroached on the white matter or cortical tracks significant enough to produce contralateral labeling of corresponding cortical areas were excluded from analysis.

Figure 2-3 was constructed by viewing adjacent sections throughout the brain with the fluorescent microscope. A score was assigned based on the relative amount of fluorescent labeling present in cortical and thalamic regions. Scores range from 0 (no label) to 3 (most densely labeled region) within brains. This scoring system is shown in Figure 2-3 as shaded boxes ranging from white (0) to black (3).

Results

Injection Sites

To describe the location of striatal injection sites and labeling in some cortical areas, it is useful to refer to landmarks external to the striatum, because of its homogeneous appearance. For this purpose, the locations of the following features, here listed in rostrocaudal order along with their shorthand designations, were used as landmarks: crossing of the genu of the corpus callosum (genu), presence of the septal nuclei without the fimbria (septum), crossing of the anterior commissure (ac), and the most rostral appearance of the fimbria distinct from the septal nuclei (fimbria). In the descriptions below these locations are referred to as the levels at which these features are seen.

The visible fluorescence of the injection sites for 10 key cases is shown in Figure 2-1. Although uptake of Fast Blue and Diamidino Yellow occurs largely, if not entirely, in the portion of the injection site that was damaged during placement of the tracer [13], I

have chosen to illustrate a larger area as a conservative estimate of the affected area. However, it is improbable that this entire visible region is producing label elsewhere in the brain [13]. These injections were all located in or around the dorsocentral region of the striatum, with variations in dorsoventral and mediolateral position. Most injection sites were elongated in the rostrocaudal dimension. Cases 5, 93 and 105 (Fig. 2-1) represent injections in mid, rostral and caudal DCS, respectively, and are presented in that order below, together with four other cases involving those regions. Cases 45 (Fig. 2-1 C,D), 52 (Fig. 2-1 F,G), 84 (Fig. 2-1 F) represent injections in dorsal DCS and these are presented separately below.

Retrograde Labeling in Cortex and Thalamus

Below are detailed descriptions of the injection sites and labeling patterns for four important cases, with the other cases discussed in reference to these.

Case 5 (central DCS). The injection site for case 5 was centered 1 mm rostral to the anterior commissure, at the level of the septum (Fig. 2-1). It was centered 700 μm ventral to the white matter, 1.5 mm lateral to the lateral ventricle, and 1.5 mm medial to the lateral boundary of the striatum. This represents an injection in the central portion of the AGm projection field in DCS. As discussed below, cases 93 and 105 represent rostral and caudal extensions (respectively) of the territory encompassed by case 5. The injection site was cylindrical and extended rostrally from its center to the level of the genu and caudally to the level of the ac.

A slight track of fluorescence lining the pipette trajectory was seen in cortical area AGl on the centermost section, but this track does not include the white matter.

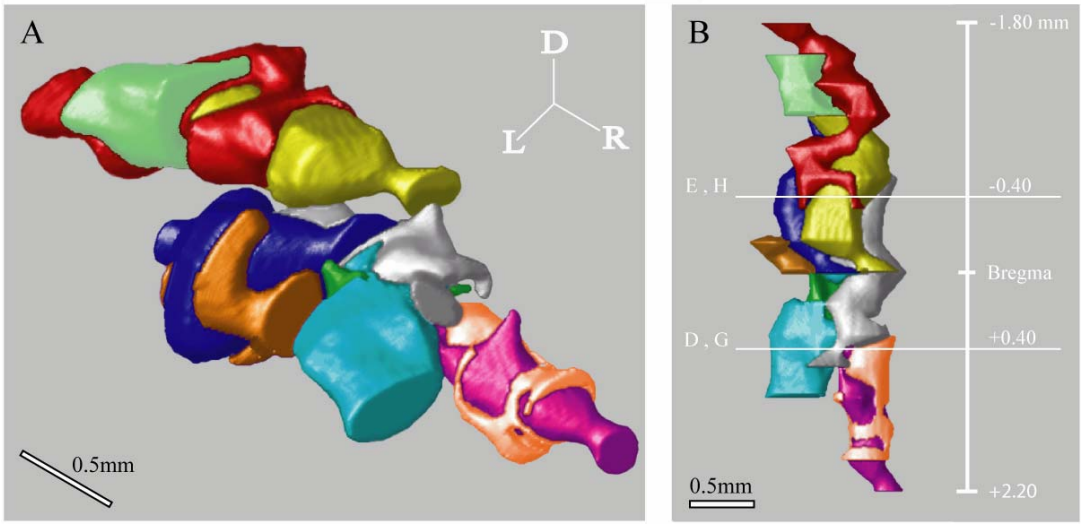

Figure 2-1. Injection sites in DCS. A) Three dimensional reconstruction of the 10 principal injection sites seen from a lateral oblique perspective, to show their relative locations within the dorsal striatum. Stick diagram indicates dorsal, lateral and rostral directions and applies to panels C and F also. B) Dorsal perspective of the same set of injections as in A, rostral toward the bottom. Vertical white line indicates rostrocaudal coordinates with respect to Bregma. Horizontal white lines indicate the plane of sections D,E and G,H. C) Three dimensional renderings of the injection sites in the four cases discussed in detail in the Results. White lines indicate the planes represented by the corresponding two-dimensional depictions of the injection sites at two levels. D-E) Location of injection sites for the four cases in C, plotted on two sections between the level of the genu and ac. Scale bar in D also applies to panels E, G and H. F) Three dimensional reconstructions of the remaining six cases. White lines indicate the planes represented by the two-dimensional depictions in G and H. G-H) Sectional views of the injections in F, at the same rostrocaudal levels as panels D and E. The injection for case 84 (light green in panel F) is not shown because it begins caudal to the level in G. Reprinted with permission from: J.L. Cheatwood, R.L. Reep and J.V. Corwin, The associative striatum: cortical and thalamic projections to the dorsocentral striatum in rats, Brain Res, 968 (2003) 1-14; Figure 1, pg 4.

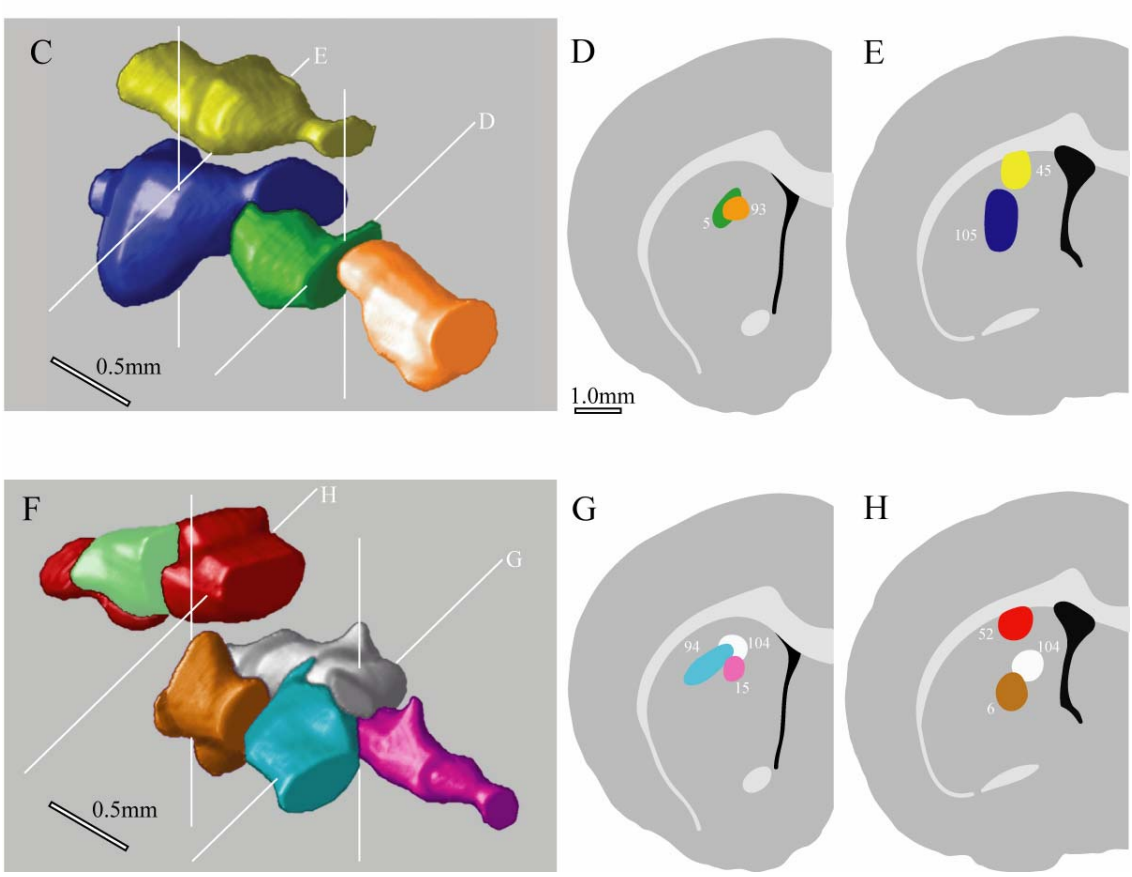

Figure 2-1. Continued

There was no label in contralateral AGl at the level of the injection, indicating that the track did not influence the labeling pattern observed. In the cortex, retrogradely labeled cell bodies were present in several areas (Fig. 2-2, Fig. 2-3). Area AGm was labeled most intensely on sections greater than 1 mm rostral to the level of the ac commissure, in layers II/III and V (Fig. 2-2 A-C). In all sections in which AGm was labeled, layer V was labeled most strongly. Areas VLO and LO were weakly labeled in layer V only. In areas PPC and Oc2M, label was only present in layer V and was most robust rostrally. In the thalamus, nuclei VL, VM, MD, the intralaminar nuclei (CM, PC, CL), and PF all contained labeled cells (Fig. 2-2 D-F). Nucleus VL appeared more strongly labeled medially than laterally, but the other nuclei were labeled throughout. The injection in case 94 overlapped that of case 5 but extended farther rostrally and lay somewhat lateral to case 5 (Fig. 2-1). Case 94 produced a broader distribution of cortical labeling (Fig. 2-3) that included all of AGm, somatic sensory and motor areas AGl, FL, HL, Par 1 and Par 2, and visual association areas Oc2M and Oc2L. The pattern of thalamic labeling was nearly identical to case 5 (Fig. 2-3).

Case 93 (rostral DCS). The injection site in case 93 was centered at the level of the genu and represents a more rostral injection than case 5, but one that is also centered in DCS. The center of the injection was located 1.1 mm ventral to the white matter. The injection was oval shaped and spanned a distance of 1.1 mm in the dorsoventral plane, 700 μm in the mediolateral plane, and 1 mm in the rostrocaudal plane. There was a very faint fluorescent track visible along the trajectory the pipette followed through AGl. Contralateral AGl contained no labeled cells. No fluorescence was evident in the white matter. Multiple cortical areas were labeled by the striatal injection.

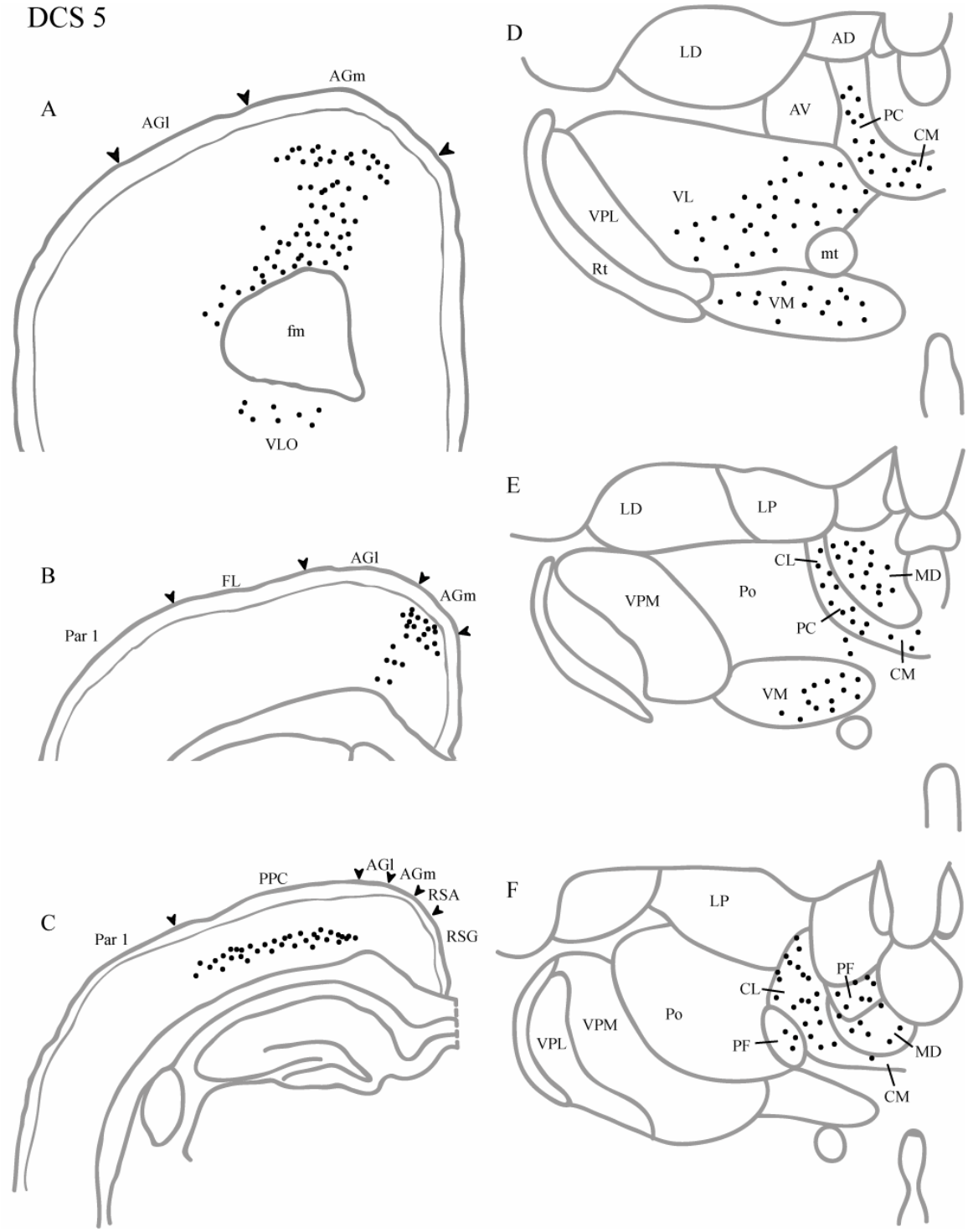

Figure 2-2. Distribution of labeled cells in case 5, an injection in central DCS, depicted on selected coronal sections through the cerebral cortex A-C) and thalamus D-F). Reprinted with permission from: J.L. Cheatwood, R.L. Reep and J.V. Corwin, The associative striatum: cortical and thalamic projections to the dorsocentral striatum in rats, Brain Res, 968 (2003) 1-14; Figure 1, pg 6.

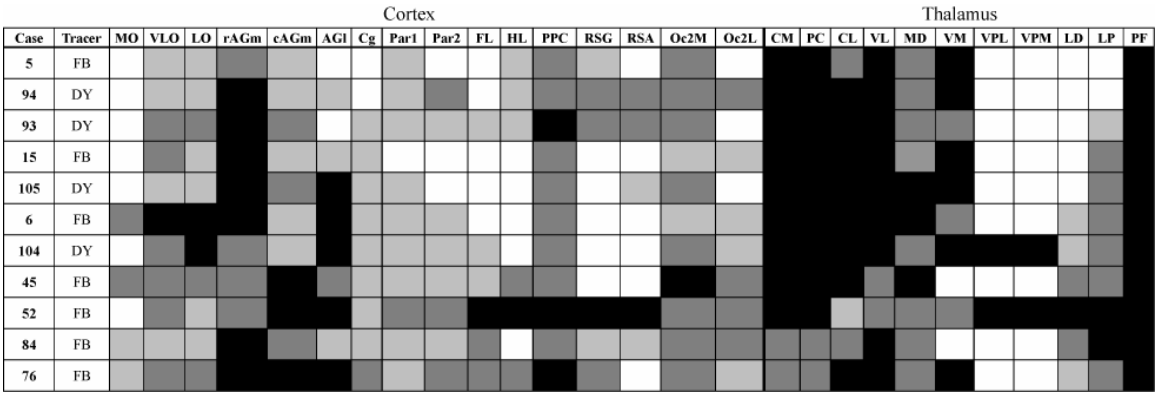

Figure 2-3. Distribution of cortical and thalamic retrograde labeling resulting from injection of Fast Blue (FB) or Diamidino Yellow (DY) in DCS and adjacent regions of the dorsal striatum. Four levels of relative labeling density are depicted: no label (white), light label (light gray), medium (dark gray), and heavy (black). Reprinted with permission from: J.L. Cheatwood, R.L. Reep and J.V. Corwin, The associative striatum: cortical and thalamic projections to the dorsocentral striatum in rats, Brain Res, 968 (2003) 1-14; Table 1, pg 3.

Labeled cells were evident in layers II/III and V of rAGm (Fig. 2-4 A,B). Label in layer V of AGm became sparser caudally and was limited to layer II/III by the level of the anterior commissure.

The labeling in layer II/III of area AGm also became less intense caudal to the anterior commissure, but remained faintly visible throughout cAGm. Label was present in layer V of area Cg at and caudal to the level of the ac. Labeled cells in area HL were limited to layer V and were present only in small numbers (Fig. 2-3B). Labeled cells in layer V of areas Oc2M, PPC, Par 1, Par 2, RSA and RSG were distributed evenly throughout their rostrocaudal extent (Fig. 2-4C,D). In the thalamus, label was observed in VL, VM, MD, the intralaminar group (CM, PC, CL), and PF with no observable topography (Fig. 2-4E,G). The injection in case 15 was virtually identical to case 93 but extended slightly more rostrally and was somewhat more focal (Fig. 2-1C,D; Fig. 2-7C). Cortical labeling was most dense in areas AGm, PPC and orbital cortex. Labeling was

dense in rAGm, sparse in cAGm. Thalamic labeling was similar to case 93, differing only in relative intensity of cellular labeling (Fig. 2-3).

Case 105 (caudal DCS). The injection site for case 105 was centered at a level 0.5 mm rostral to the ac, and represents a location caudally adjacent to case 5 (Fig. 2-1, Fig. 2-7A). The center of the injection was located 1 mm ventral to the white matter and 1.1 mm lateral to the lateral wall of the lateral ventricle. The injection measured 1.4 mm in the dorsoventral plane, 600 μm in the mediolateral plane, and 1.5 mm in the rostrocaudal plane (it extended from 500 μm caudal to the level of the genu to the level of the ac). There was no evidence of fluorescent tracer lining the path through which the pipette was inserted, nor was there any fluorescent material in the white matter. In the cortex, several areas contained labeled cells. Areas VLO, LO, and the rostral portions of AGm and AGl contained labeled cells in layers II/III and V (Fig. 2-5A,B). Area AGm remained labeled throughout its rostrocaudal extent and densely in cAGm, though layer V was no longer labeled caudal to the level of the ac. Labeled cells in area AGl were seen only until the level of the ac. Label was observed in area Cg at the level of the ac and continued to its caudal boundary. Areas HL, PPC, Oc2M, Par 1, Par 2, and PRh all contained labeled cells in layer V throughout their rostrocaudal extents (Fig. 2-5C,D). In the thalamus, nuclei AV, VL, VM, the intralaminar nuclei (CM, PC, CL), MD, PF, and rostral LP all contained labeled cells (Fig. 2-5E,G).

The injection in case 6 partially overlaps that of case 105 throughout most of its extent, but is centered more ventrally (Fig. 2-1; compare panels D and G).

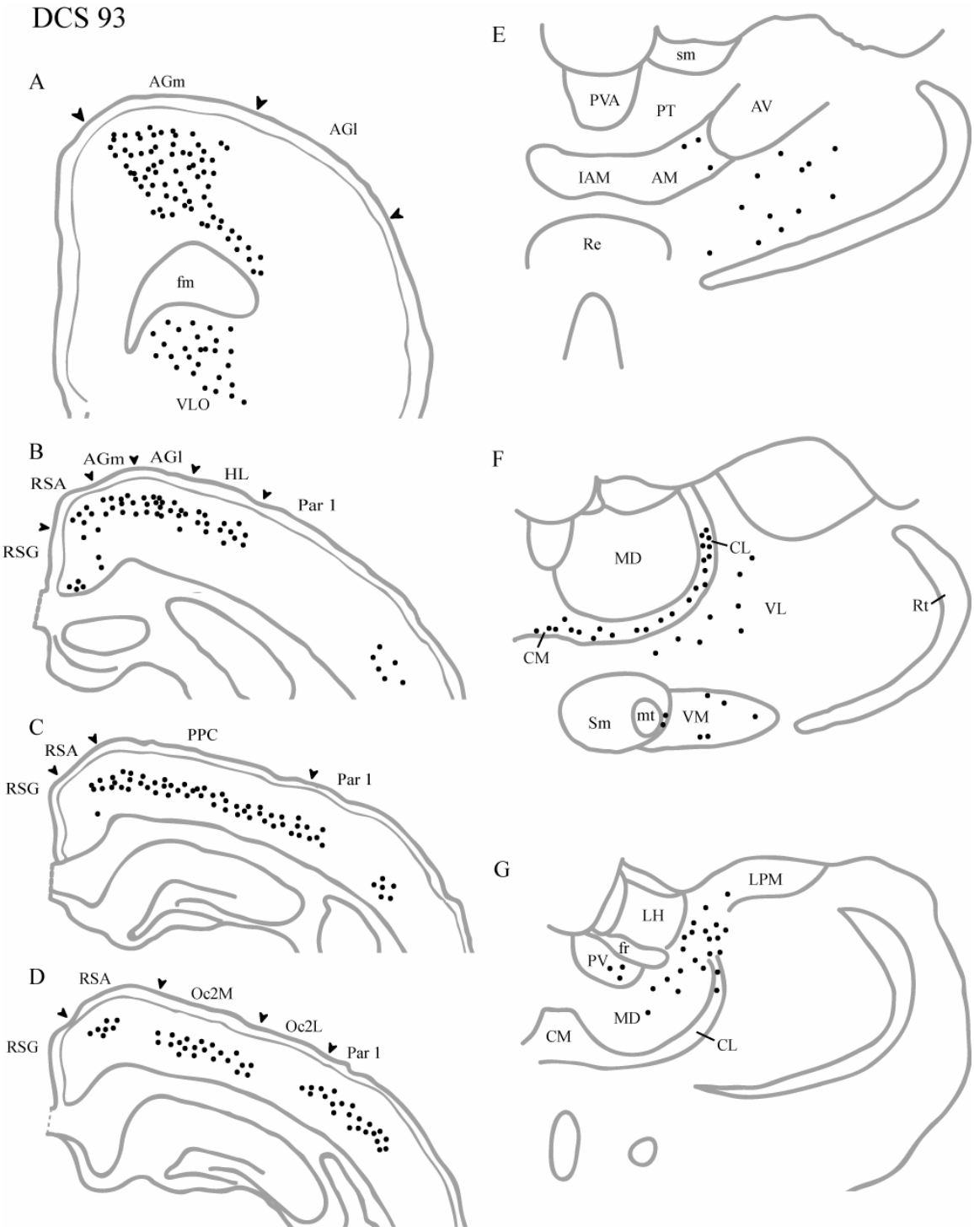

Figure 2-4. Distribution of labeled cells in case 93, an injection in rostral DCS, depicted on selected coronal sections through the cerebral cortex A-D) and thalamus E-G). Reprinted with permission from: J.L. Cheatwood, R.L. Reep and J.V. Corwin, The associative striatum: cortical and thalamic projections to the dorsocentral striatum in rats, Brain Res, 968 (2003) 1-14; Figure 3, pg 7.

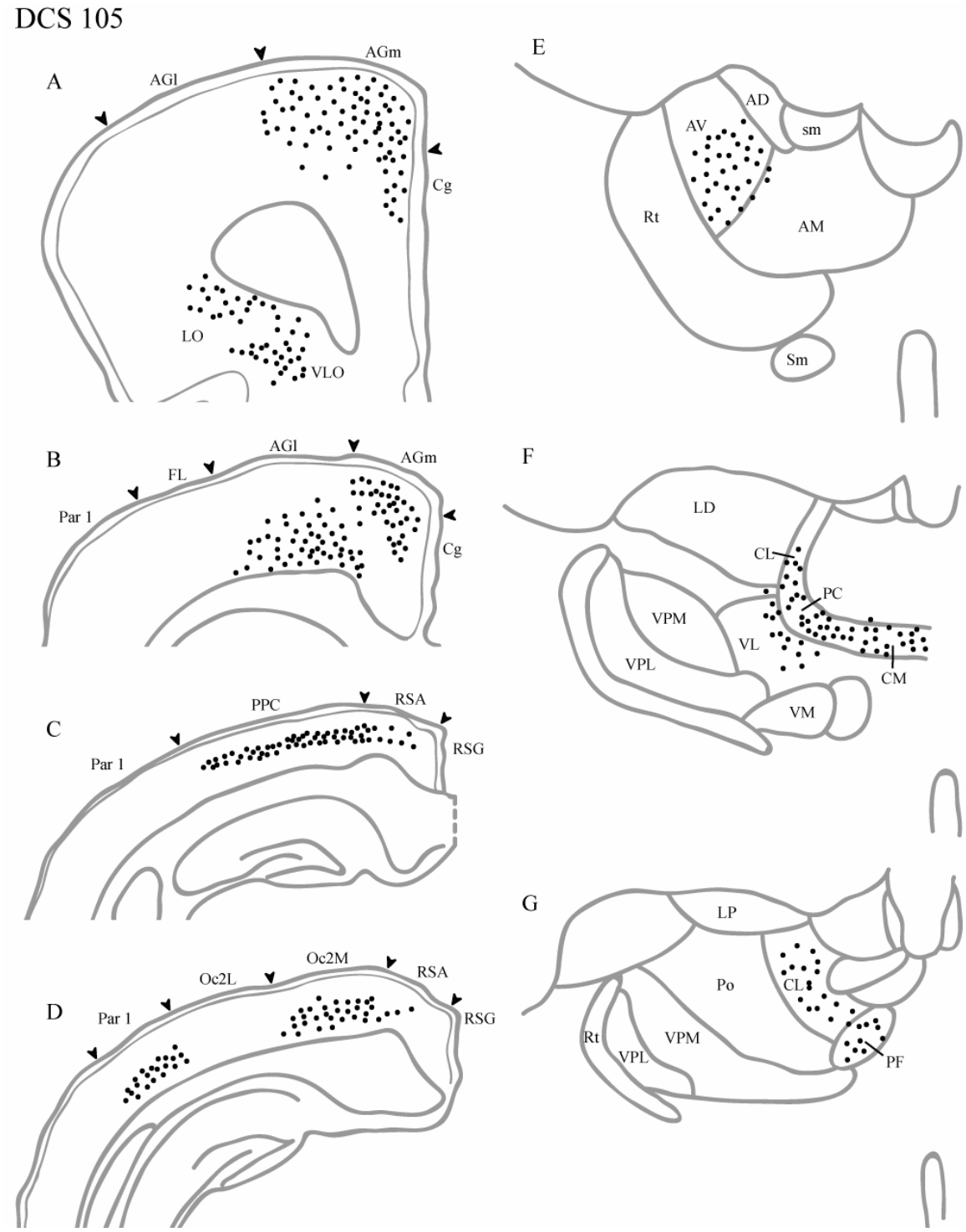

Figure 2-5. Distribution of labeled cells in case 105, an injection in caudal DCS, depicted on selected coronal sections through the cerebral cortex A-D) and thalamus E-G). Reprinted with permission from: J.L. Cheatwood, R.L. Reep and J.V. Corwin, The associative striatum: cortical and thalamic projections to the dorsocentral striatum in rats, Brain Res, 968 (2003) 1-14; Figure 4, pg 8.

Cortical labeling included many of the same areas as in case 105 but AGm was labeled more intensely in rostral portions and somatic sensorimotor labeling did not include area HL. Thalamic labeling was very similar to case 105 with the addition of labeling in LD (Fig. 2-3).

Case 104 had an injection site located just medial to that of case 105 (Fig. 2-1). It also extended more rostrally than case 105. These two injections overlap partially in the middle of their a-p ranges. The pattern of cortical labeling for case 104 is similar to the pattern seen in case 105, with the addition of labeling in areas FL, Par2, and Oc2L, and a lack of labeled cells in RSA. Thalamic labeling differed from case 105 in the addition of LD, VPL, and VPM (Fig. 2-3).

Case 45 (dorsal DCS). The injection site in case 45 was centered at the level of the anterior commissure and extended caudally to the level of the fimbria (Fig. 2-1). The injection was spherical in shape and measured 500 μm in diameter. The dorsal border of the injection lay against the ventral border of the white matter. Therefore, this case represents a dorsal injection with respect to the boundaries of DCS. A moderate fluorescent track outlining the path of the pipette could be seen in all layers of area FL immediately above the center of the injection. Contralateral FL was not labeled, indicating that the track did not cause a change in the labeling pattern of the striatal injection. Because of the location of the injection site, a slight amount of fluorescence was visible in the white matter. In the cortex label could be seen in areas AGm, AGl, PPC, Oc2M, Oc2L, Par 1, Par2, MO, VLO, LO, Cg, FL, HL, and PRh. Throughout its extent area AGm was labeled most densely in layers II/III, with infrequent labeling in layer V. Fluorescence was strongest within 1 mm of the ac (Fig. 2-6A,B). Labeled cells

in layer V of area AGl could be seen from the level of the anterior commisure through the caudal border of AGl. Area PPC contained numerous labeled cells in layer V throughout its extent (Fig. 2-6C). Label in layer V of areas Oc2M and Oc2L began at their rostral pole and continued caudally through the remaining sections (Fig. 2-6D). Area Par 1 contained lightly labeled cells in layer V only (Fig. 2-6C,D). Perirhinal cortex contained labeled cells in layer V only. In the thalamus, nuclei AV, AD, VL, LD, medial LP, the intralaminar nuclei (CM, PC, CL), and PF contained labeled cells throughout their extent. Thalamic nucleus MD was labeled more strongly rostrally (Fig. 2-6E,G).

Case 52 had an injection site that overlapped that of case 45 from the level of the ac to the level of the fimbria, but extended more caudally (Fig. 2-1). Cortical labeling differed from case 45 by being sparse in rAGm, absent in MO, and present in areas RSA and RSG. In the thalamus the distribution was identical to case 45, with the addition of robust labeling in nuclei VPM and VPL (Fig. 2-3).

Case 84 had an injection site located lateral to both cases 45 and 52, and mostly caudal to case 45 (Fig. 2-1). Cortical labeling was similar to case 45 with the addition of labeled cells in RSA and RSG, and an absence of label in HL. The thalamic pattern was the same as case 45 (Fig. 2-3, Fig. 2-7D).

Case 76 (Fig. 2-7B) involved a large injection that was dorsally located but did not overlap with the more caudal dorsal injections represented by cases 45, 52 and 84. It did overlap significantly with several rostral injections including cases 5, 15, 93, 94 and 104. Cortical labeling was extensive but excluded Par 1 and Par 2 (Fig. 2-3). The thalamic labeling pattern was similar to the other dorsal cases presented above (Fig. 2-3).

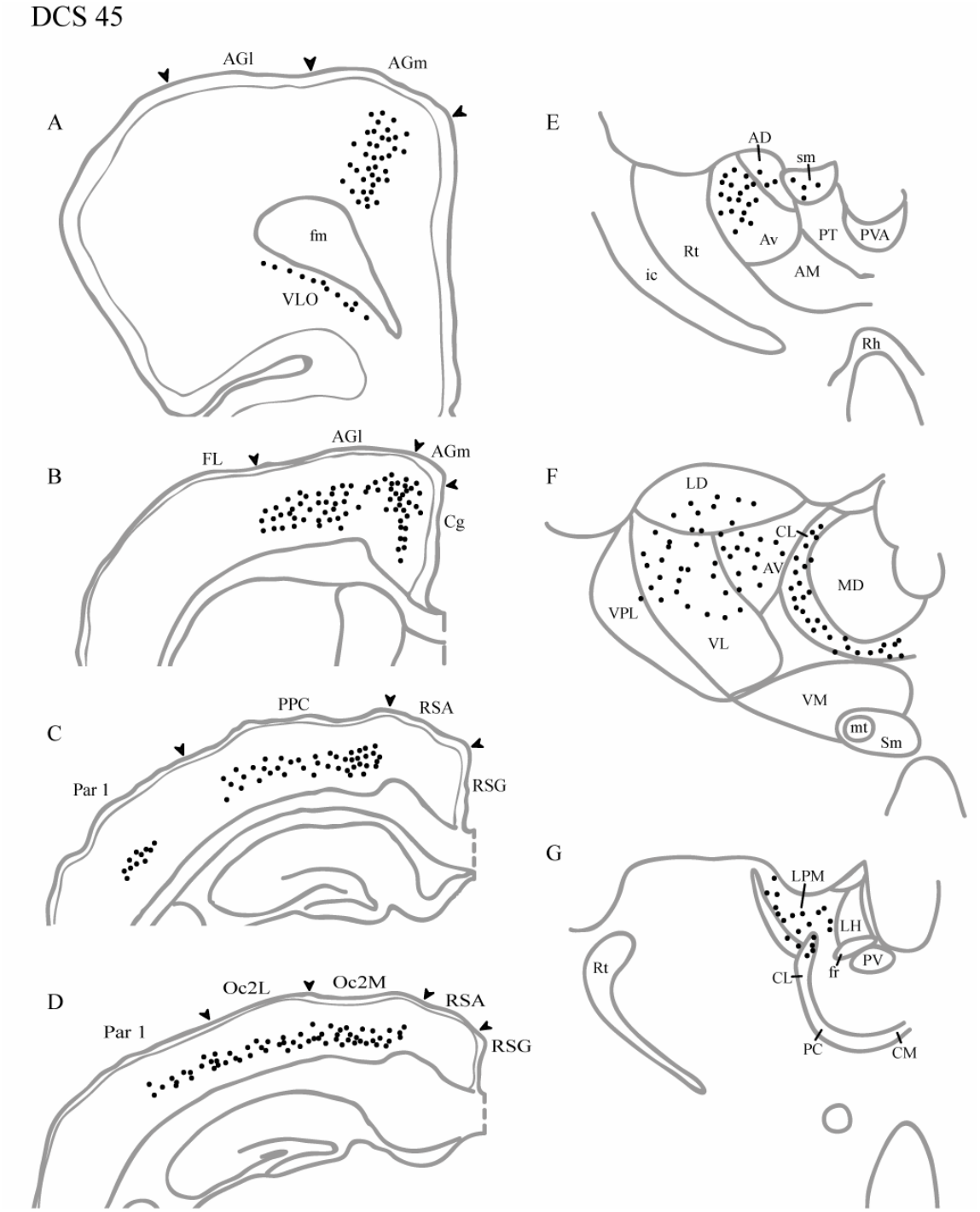

Figure 2-6. Distribution of labeled cells in case 45, depicted on selected coronal sections through the cerebral cortex A-D) and thalamus E-G). Reprinted with permission from: J.L. Cheatwood, R.L. Reep and J.V. Corwin, The associative striatum: cortical and thalamic projections to the dorsocentral striatum in rats, Brain Res, 968 (2003) 1-14; Figure 5, pg 10.

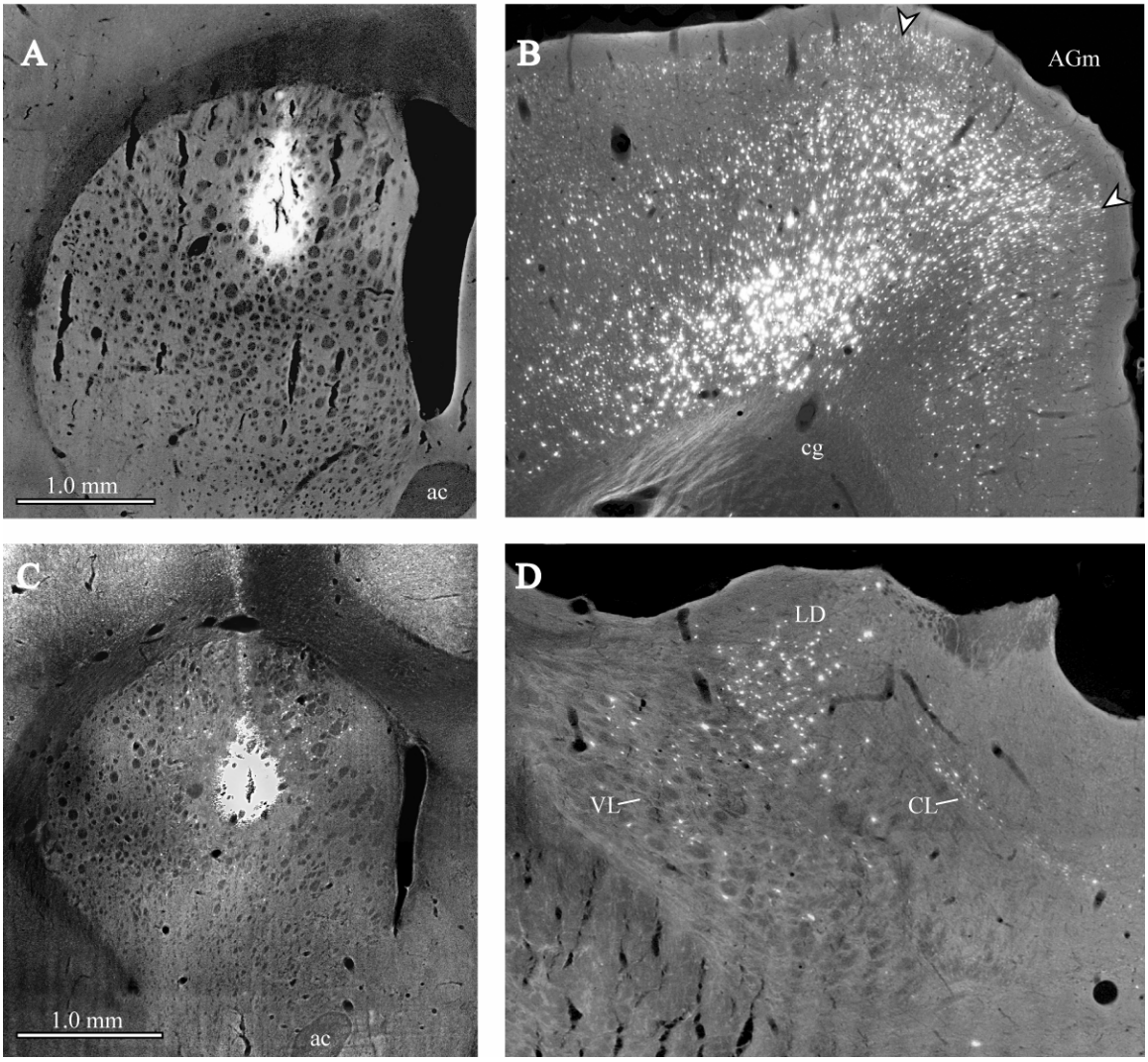

Figure 2-7. Fluorescent photomicrographs of representative sections from select cases. A) The Diamidino Yellow (DY) injection site in case 105 at the level of the septum. B) Retrograde labeled cells in cortical area AGm, case 76. C) The Fast Blue (FB) injection site in case 15 at the level of the genu. D) Retrograde labeled cells in the thalamus, case 45. Reprinted with permission from: J.L. Cheatwood, R.L. Reep and J.V. Corwin, The associative striatum: cortical and thalamic projections to the dorsocentral striatum in rats, Brain Res, 968 (2003) 1-14; Figure 6, pg 11.

Topography

From the cases presented above it was possible to discern some topographic patterns of connectivity. With regard to the cortex it is notable that all injections produced labeled cells in areas AGm, PPC, orbital cortex, and Oc2M. No other cortical areas were labeled with this degree of consistency. The pattern of labeling in AGm was correlated with the location of the injection in DCS. Most of the injections had a longer rostrocaudal than dorsoventral extent and produced at least some labeling across the full rostrocaudal extent of areas AGm and PPC. However, injections centered rostrally in DCS (cases 5, 15, 93, 94) tended to produce their most robust labeling in rAGm whereas injections located in caudal DCS (cases 70104, 105) exhibited sparser labeling in rAGm. One important exception is case 6, which had an injection located more ventrally in caudal DCS than cases 104 and 105, and exhibited only slight labeling in cAGm. Area PPC and visual association cortical areas Oc2M and Oc2L were labeled most densely in cases with injections on the dorsal border of DCS (cases 45, 52, 76, 84) and those placed caudally in DCS (104, 105). A rostrocaudal pattern of topography was also noticeable to a lesser degree in area AGl.

In the thalamus, the nuclei with the most evident topographical relationship with striatum were LD and LP. Labeled cells were found in LD and LP only in cases with injections in dorsal portions of DCS.

Discussion

Two important findings of the present study are the identification of cortical areas that project to DCS, and the discovery of a high degree of overlap in the projections from AGm and PPC. Also of significance is the finding that the thalamic nuclei projecting to

DCS are also those that project to the cortical areas that provide input to DCS. Finally, there is evidence of some topography within DCS.

Corticostriatal Connections

Many cortical areas have some projections to DCS but the most frequent contributors are areas AGm, AGl, PPC, VLO, LO, and Oc2M. The projections from AGm and other frontal cortical areas to the striatum are arranged along rostrocaudal and mediolateral gradients [5,6,30,93], and the rostrocaudal topography observed in the present study with regard to the projections from AGm is consistent with these previous reports. There is also evidence of dorsoventral topography with respect to the labeling pattern in AGm. The injection in case 6 was the most ventral in the sample, and produced very little labeling in cAGm. This is consistent with the fact that cAGm projects to a more dorsal region within caudal DCS [93].

Evidence for spatial overlap in the terminal fields of axons projecting from AGm and PPC to the striatum was noted previously [93,97]. In the present cases, all injections produced some degree of labeling in both PPC and AGm, confirming the previous anterograde findings based on single injections in different brains. This finding is in itself suggestive of a potential relationship between information coming from AGm and PPC into DCS, and relates to functional studies demonstrating that AGm and PPC are parts of an interconnected network mediating spatial processing and directed attention [15]. This network also includes orbital cortex and Oc2M, the final two regions labeled in every brain.

The present retrograde findings demonstrating convergence in the region of DCS of inputs from AGm, PPC and orbital cortex at the light microscopic level are suggestive of a possible interaction among these inputs. In primates, Yeterian and Van Hoesen

[136] first demonstrated convergent striatal projections from distant cortical areas and related this to the corticocortical connectivity between these areas. A later study by Selemon and Goldman-Rakic [104] showed that most convergence of this kind actually consist of zones of interdigitating projections rather than true overlap, and that convergence occurs even among projections from cortical areas that are not themselves interconnected. In rodent somatic sensory striatum there is significant true overlap in addition to interdigitation in the case of projections from cortical barrels representing the same whisker row [3]. It is possible that AGm, PPC, and VLO each project to a discrete territory within DCS, with little or no overlap. Alternatively, there may be convergence onto single striatal neuron dendritic trees [133]. These issues are discussed in more detail in a companion study [92], which found that dense patches of segregated labeling from AGm and PPC are interspersed with less dense patches of overlapping label in DCS.

The convergence in DCS of input from AGm and PPC is also interesting because of behavioral and pharmacological data implicating DCS as a critical site necessary for normal directed attention and spatial processing, and recovery from deficits induced by cortical lesions [115,116]. The cannula placements in these studies tended to involve the dorsal portion of DCS between the levels of the septum and ac, exactly that territory implicated by the present findings as the AGm-PPC overlap zone.

In the present study visual association areas Oc2m and Oc2L were consistently labeled most densely with dorsal and caudal injections, and this is consistent with the topography defined by others [72,76]. No labeling was seen in area Oc1, which projects to a circumscribed region of dorsomedial striatum bordering the lateral ventricle [72], outside the injected territory. These authors noted that areas Oc2M and Oc2L project not

only to this dorsomedial sector but also to the more deeply located territory encompassed by the current injections, which is consistent with the current findings.

Several other cortical areas labeled by injections in DCS have their densest corticostriatal terminations outside of DCS. Physiologically identified motor areas for the forelimb and hindlimb project in a banded pattern to the dorsolateral striatum but the less dense medial portions of their projection fields appear to be located on the lateral margin of DCS [30]. The physiologically identified vibrissal-eyefield area located in AGm projects in a topographic manner to DCS and a dorsolateral shell [30]. Somatic sensory areas also project most densely to the dorsolateral striatum in banded patterns [10,50], but in each case the medial-most band is located within DCS between the levels of the genu and ac [10]. The focal size of these medial bands together with individual variation may explain the variability observed in labeling of somatic sensory areas. Orbital and cingulate cortical areas project to territories along the ventral and medial borders of DCS and appear to have their densest terminations outside of DCS [5,6].

Some discrepancies observed in the present study may relate to the focal, distributed nature of corticostriatal axon arborizations [4,17,60,61,71] and their potential for variability across individuals. Cases 15 and 93 appeared to occupy virtually overlapping regions but there was more widespread cortical labeling in case 93. Likewise, the dorsal cases 45, 84, and 76 exhibited labeled cells in orbital area MO; cases 52 also a dorsal injection, but did not produce labeling in MO.

The laminar distribution of labeled cortical neurons varied across cortical areas and within AGm. Labeled neurons were present in layers II/III and V in AGm and AGl but only in layer V of the other cortical areas. Within AGm it was common to find only

layers II/III labeled caudal to the level of the ac, as described for cases 93, 105 and 45. Wilson [131] also reported labeling in layers II/III and V within ipsilateral AGm, and labeling restricted to layer V in somatic sensory cortex following injection of a retrograde tracer into the striatum.

Due to the long rostrocaudal extent of the current injections, the ability to make statements about highly discrete topography of cortical projections to DCS is limited. The observed rostrocaudal expansion of the injections could be due to diffusion along corticostriatal axons, which are known to traverse long distances in the striatum, synapsing on striatal neurons at varying rostrocaudal levels [54]. Selemon and Goldman-Rakic [104] demonstrated that some cortical areas project axons that traverse the entire rostrocaudal extent of the primate caudate nucleus. Diffusion of this type presents a unique problem for discrete retrograde analyses in DCS and should be addressed in future studies.

Similarly, the placement of a tracer in the rat striatum raises the possibility of uptake not only by the axons of interest but also those fibers that are only passing through the striatum to form terminals elsewhere in the CNS. This is known to occur with retrograde fluorescent tracers [13]. However, the coordinated pattern of thalamic and cortical labeling suggests uptake by axon terminals, because it seems unlikely that interconnected cortical and thalamic regions would be consistently labeled via uptake by fibers of passage. Rather, it would appear more parsimonious to suggest that the axons from such linked cortical and thalamic regions terminate in the same striatal territory. Ultimate resolution of this question will depend on double anterograde tracing.

Thalamostriatal Projections

The pattern of thalamic projections to DCS bears a striking resemblance to the thalamic projections to those cortical areas that provide input to DCS. The rostral portion of area AGm receives thalamic input from lateral MD, VL, VM and the intralaminar nuclei, whereas inputs to caudal AGm emphasize VL, LD, LP and Po [49,93,94]. In the present study these same thalamic nuclei were found to project to DCS, with the exception of Po and the addition of the parafascicular nucleus. It is known that single neurons of the central lateral nucleus project to both the striatum and cortex [21], and if this is also an attribute of the projections of the other thalamic nuclei projecting to DCS it could underlie the registration observed. Anterograde tracing has demonstrated that the intralaminar nuclei (CM, PC, CL) have dense projections to the dorsal striatum [7,8]. Although their terminal fields are generally located medially (CM), centrally (PC) and laterally (CL), they overlap to some extent in the dorsocentral striatum, especially rostral to the level of the ac. This may explain why all three nuclei were labeled in all of the current cases.

There is evidence of topography in the thalamic projections to DCS from LD and LP, and the observed pattern is consistent with the known organization of thalamocortical projections involving these nuclei and the topography of corticostriatal projections from their cortical targets. Injections in dorsal DCS consistently labeled thalamic nuclei LD and LP. Together with the fact that LD and LP project to cAGm [93], this topography suggests that dorsal DCS is preferentially related to cAGm. Consistent with this claim, corticostriatal projections from cAGm project most densely to dorsal DCS [93]. Thalamic nuclei LD and LP also project to cortical areas PPC and Oc2M [91], which are densely connected with cAGm rather than rAGm [91,97]. Finally, cortical input to dorsal

DCS is densest from areas PPC and Oc2M (present study and [92]; see Chapter 3). Thus, dorsal DCS appears to represent a subregion of DCS that is distinguished by its network of thalamic and cortical connections. As an aside, the projections from LP to DCS and AGm [93,109] originate predominately from its medial portion, whereas the projection from LP to area PPC originates from all of LP [91].

The current results are in agreement with the topography of labeling produced following injections of retrograde tracers (Fluorogold and the cholera toxin ß-subunit) into the dorsomedial caudate-putamen, with the addition of AV and AD labeling [31]. The description of the rostrocaudal and mediolateral topography of labeled cells in the lateral and ventral thalamic nuclei following injections in the Erro *et al*. paper is consistent with the pattern of labeling produced in the current cases. They reported labeled cells in the ipsilateral intralaminar nuclei and medial thalamic nuclei in all of their cases [31]. Additionally, Erro *et al*. note that they found labeled cells in VPM and VPL following injections in the caudal striatum, a feature that is not widely accepted. The current injections also produced robust labeling in VPM and VPL in some, but not all, caudal (postcommisural) injections [31].

Conclusions

The present results together with previous findings demonstrate that DCS receives input from cortical and thalamic regions that are themselves interconnected. Furthermore, DCS and connected cortical areas are involved in directed attention and its dysfunctional counterpart, multimodal hemispatial neglect. The data presented herein suggest that DCS is a key element of a cortico-striatal-thalamic network specialized for multimodal associations and spatial functions including directed attention. This network includes cortical areas AGm and PPC, the striatal area DCS, and the thalamic nuclei VL,

MD, LD, LP, and the intralaminar group. This network is similar to the large scale networks proposed to be involved in spatial functions in primates [48,77,105]. Similar interconnected cortico-striatal-thalamic networks have been identified for sensory, motor and limbic systems [1,46,85].

CHAPTER 3
OVERLAP AND INTERDIGITATION OF CORTICOSTRIATAL AFFERENTS TO DORSOCENTRAL STRIATUM IN THE RAT

Introduction

Using a rodent model of hemispatial neglect [62-64,92,115-118], our group has determined that the medial agranular cortex (AGm), a multimodal association premotor cortex with diverse cortical connections [97], and posterior parietal cortex (PPC) are components of a cortico-striato-thalamo-cortical network mediating directed attention in the rat [16]. The dorsocentral striatum (DCS), defined anatomically as the central striatal terminal field of projections originating from cortical area AGm, is critical for normal directed attention. Destruction of DCS results in chronic neglect which does not recover or respond to dopamine agonists [93,115-117]. For these reasons, region DCS has become the focus of work on the cortical-striatal-thalamic network mediating directed attention in the rat.

In previous anterograde and retrograde studies, we demonstrated that the cortical regions AGm, PPC, ventrolateral orbital cortex (VLO), and secondary visual cortex (Oc2M) all send projections to each other and to DCS [16,93,92]. Projections from each of these areas form a dense primary projection field in the dorsal striatum and an additional diffuse pattern of labeling in or near DCS. This pattern of labeling in the rat striatum has been described by many authors [3,10,51,74,92,134], and suggests the presence of at least two systems of corticostriatal projections terminating in the rat striatum, termed “discrete” and “diffuse” [134]. The same diffuse region of

corticostriatal labeling was also described in the monkey [34,35], and may therefore be an innate property of corticostriatal organization. A thorough examination of the band/diffuse pattern of labeling in the rat network for directed attention was recently published by Reep and colleagues [92].

Previously, the thalamic nuclei with which the cortical components of the rat network for directed attention are each reciprocally interconnected were identified [93]. Because of the known functional and anatomical relationships between cortical areas and thalamic nuclei in the network [65,91,93,96,97], it is important to understand the topography of their striatal projections and the spatial relationship of these projections with respect to DCS. More detailed examination of the relationship between the convergent terminal fields of these key regions will provide a better basis to understand how their inputs interact to influence the activity of neurons in the DCS. Cortico-striato-thalamo-cortical networks have also been proposed as mediators of directed attention in primates. Similar to the rat network, the primate networks involve regions of prefrontal cortex and posterior parietal cortex, as well as associated regions of the basal ganglia and thalamic nuclei [73,77,105].

Interest in these specific cortical areas extends to the more general question of whether multiple cortical areas terminate on or near the dendrites of individual striatal medium spiny neurons. This hypothesis has been proposed previously [136] and is supported by both electrophysiological and anatomical data [17,33,80], although it remains untested in a multi-labeling experiment at the light microscopic level. If it exists, this pattern of connectivity would support the hypothesis that the rat striatum, and potentially individual medium spiny neurons, plays a key role in integrating multimodal

input from diverse cortical areas, and that the rat DCS is a center for convergence of diverse corticostriatal inputs related to directed attention. Previous reports support these hypotheses. In Chapter 2, I found that many cortical areas project to region DCS, but none more consistently than AGm, PPC, and Oc2M. Subsequently, we demonstrated that axons from cortical areas AGm and PPC exhibit both overlap and interdigitation in the rat DCS, using an anterograde tracer placed in individual cortical areas, as well as in two double-labeled cases [92].

In the current multiple-labeling study we directly tested the hypothesis that projections from cortical areas PPC and VLO, as well as thalamic nuclei VL and LD, overlap and/or interdigitate with projections from cortical area AGm in the striatal region DCS. Further, I sought to demonstrate whether neurons from anatomically non-adjacent cortical areas form terminals on or near the dendrites of the same individual medium spiny neurons in the rat striatum.

Materials and Methods

All animal procedures were conducted according to institutional protocols that meet or exceed NIH and Society for Neuroscience guidelines. Animals were anesthetized with ketamine/xylazine (90mg/kg:10mg/kg). Upon cessation of tail pinch and eyeblink responses, animals were placed in a small animal stereotaxic device and holes were drilled in the skull at the selected location. The dura was then incised, exposing the brain surface. All rats received one injection of a 10,000mw dextran conjugated to a green-fluorescing molecule (100nl of a 10% AlexaFluor 488 solution in phosphate buffer; Molecular Probes, Inc.) in area AGm using procedures derived from previous work by the Reep group [91,92,97]. Additionally, each rat received an injection of a red fluorescing molecule conjugated to a 10,000mw dextran (100nl of a

10% FluoroRuby or MicroRuby solution in phosphate buffer; Molecular Probes, Inc.) in one of the following regions: cortical area AGl (case DCS 193), PPC (case DCS 178), VLO (case DCS 147), or thalamic nucleus VL (case DCS 173), or LP (case DCS 191). One rat (case DCS 193) also received a third injection: a 3,000mw dextran conjugated to a biotin molecule (BDA3K; Molecular Probes) was placed in globus pallidus and retrogradely filled the dendritic trees of medium spiny neurons in DCS.

Injections for all cases were placed in the left hemisphere. Intracerebral injections were made through a 27-gauge Hamilton syringe except for injections in orbital cortex, which necessitated the use of iontophoresis. For iontophoretic injections, glass micropipettes having tip diameters of 20-30 µm were lowered to the proper coordinates and constant current pulses of 4-5 µA were delivered from an iontophoresis unit (Kation Scientific, model BAB-350) in a 5 sec on/5 sec off pattern for 20-25 minutes. All thalamic injections were made iontophoretically using the same parameters as cortical iontophoretic injections. After surgical procedures were completed, all skull wounds were filled with gelfoam and antibiotic ointment was placed between the scalp and skull to prevent post-surgical infection. The scalp wound was closed using wound clips. After 10-14 days rats received an overdose of a barbiturate solution (Beuthanasia-D; 100mg/kg IP) and were perfused intracardially with 34^{o}C phosphate-buffered saline followed by 4% phosphate-buffered paraformaldehyde. The brain was extracted and post-fixed in 4% paraformaldehyde fixative for 24hr, then stored in cold 0.4% paraformaldehyde containing 30% sucrose for 2-3 days prior to cutting.

Coronal frozen brain sections were cut at 40 µm on a sliding microtome and collected serially in dilute fixative (0.4% paraformaldehyde). Two series of sections

were mounted, dehydrated and coverslipped using Fluoromount (BDH Chemicals). Fluorescent sections were viewed and photographed on a Biorad MRC-1024 confocal laser scanning microscope using separate red and green filter channels. Final images represent combined red/green image stacks of approximately 20 μm total thickness.

A third series of sections stored in dilute fixative was stained for Nissl substance using cresyl violet and used for cytoarchitectural orientation. Additionally, brains containing microruby or BDA3K injections were processed as previously described [92].

The locations of cortical injection sites were determined in each brain according to the cytoarchitectural criteria of Zilles and Wree [137]. The terms AGm and AGl are synonymous with their areas Fr2 and Fr1, respectively. Thalamic nuclei were identified and demarcated according to the criteria and maps of Jones [53] and Paxinos and Watson [87].

Data from single anterograde biotinylated-dextran-amine (BDA) injections are previously unreported findings resulting from a reanalysis of 13 rats for which methods were previously reported, as were the methods for calbindin staining on those cases [92]. For the purpose of this report, only rats with injections which affected only one cortical area were analyzed.

Results

Injections of anterograde fluorescent tracers in AGm (green) and a second brain region (red) resulted in the simultaneous red and green labeling of terminal fields in the striatum. I attempted to determine whether the striatal terminal fields labeled by each tracer injection overlapped or interdigitated. As noted previously, I viewed the sections on a confocal microscope and imaged ~20μm of each ~40μm-thick section in ~1μm intervals. The images from each stack were combined via software into one two-

dimensional image. Therefore, axons seen to cross on final images are somewhere between actually touching and passing within 20μm of one another. Since the two conditions are indistinguishable on the final images, I considered any image in which fibers from different injections were observed crossing as an image depicting overlap. "Interdigitation" was used to describe sections on which very little or no overlap was seen, yet axons from different injection sites (typically large fields of them) were seen adjacent to one another.

Placement of injection sites is described below in anteroposterior (a-p), mediolateral (m-l), and dorsoventral (d-v) dimensions.

Injections in AGm/AGl

In case DCS 193, the AGm injection was centered at a-p +1.0 and affected an area similar to the injection in case 178, extending to all cortical layers without damaging the white matter. The AGl injection was centered at a-p -3.6 and m-l +2.0, and affected all cortical layers, as well as a small amount of the white matter. The AGm labeling in case 193 produced a dorsolateral band and DCS labeling consistent with the previous accounts [92]. A dorsolateral band of labeling was produced in the striatum following the AGl injection, and sparse axonal labeling was observed in DCS, as previously described [92]. The dorsolateral band is distinct from the AGm band, but labeling in DCS overlapped with AGm labeling.

Additionally, case DCS 193 also received an injection of BDA3K in globus pallidus (a-p -0.9), resulting in a robust retrograde labeling of the DCS efferent neurons (medium spiny neurons). With confocal microscopy, both green (AGm) and red (PPC) fine-caliber axons with varicosities were observed to overlap with individual dark-stained medium spiny neuron dendrites in this triple-labeled brain (Figure 2C,2D).

Injections in AGm/PPC

Case DCS 178 received fluorescent tracer injections in cortical areas AGm and PPC and both produced a pattern of labeling in the striatum similar to those seen previously after single injections of the anterograde tracer BDA [92]. The AGm injection site was centered at a-p +0.7 and affected all cortical layers but did not affect the white matter (Fig 3-1A). Terminal fields from area AGm included a dorsolateral band immediately internal to the white matter, as well as a more diffuse area of labeling in DCS, as reported previously [92,93]. The PPC injection site for case 178 was centered at a-p -3.6 (Fig 3-1B), and affected all layers of the cortex without extending into the white matter. The injection is centered in PPC and has a narrow mediolateral extent (~0.2mm). The injection is visible over a rostrocaudal distance of approximately 0.3mm (from spaced serial sections). The primary terminal field of projections from area PPC forms a dense band located dorsal to the AGm projection field in DCS, and it spans the distance between DCS and the dorsolateral AGm band but remains distinct from both fields of AGm axon terminals. The same pattern of termination can be observed along much of the rostrocaudal extent of the striatum in this case.

In case 178, the PPC injection also produced a dense focus of labeling in DCS (Fig 3-2A,B). The focal PPC projection in DCS was somewhat distinct from AGm labeling in its center but overlapped extensively with AGm axons at the edges of the focus. Numerous axons from each injection were observed in the focus periphery and crossed each other extensively.

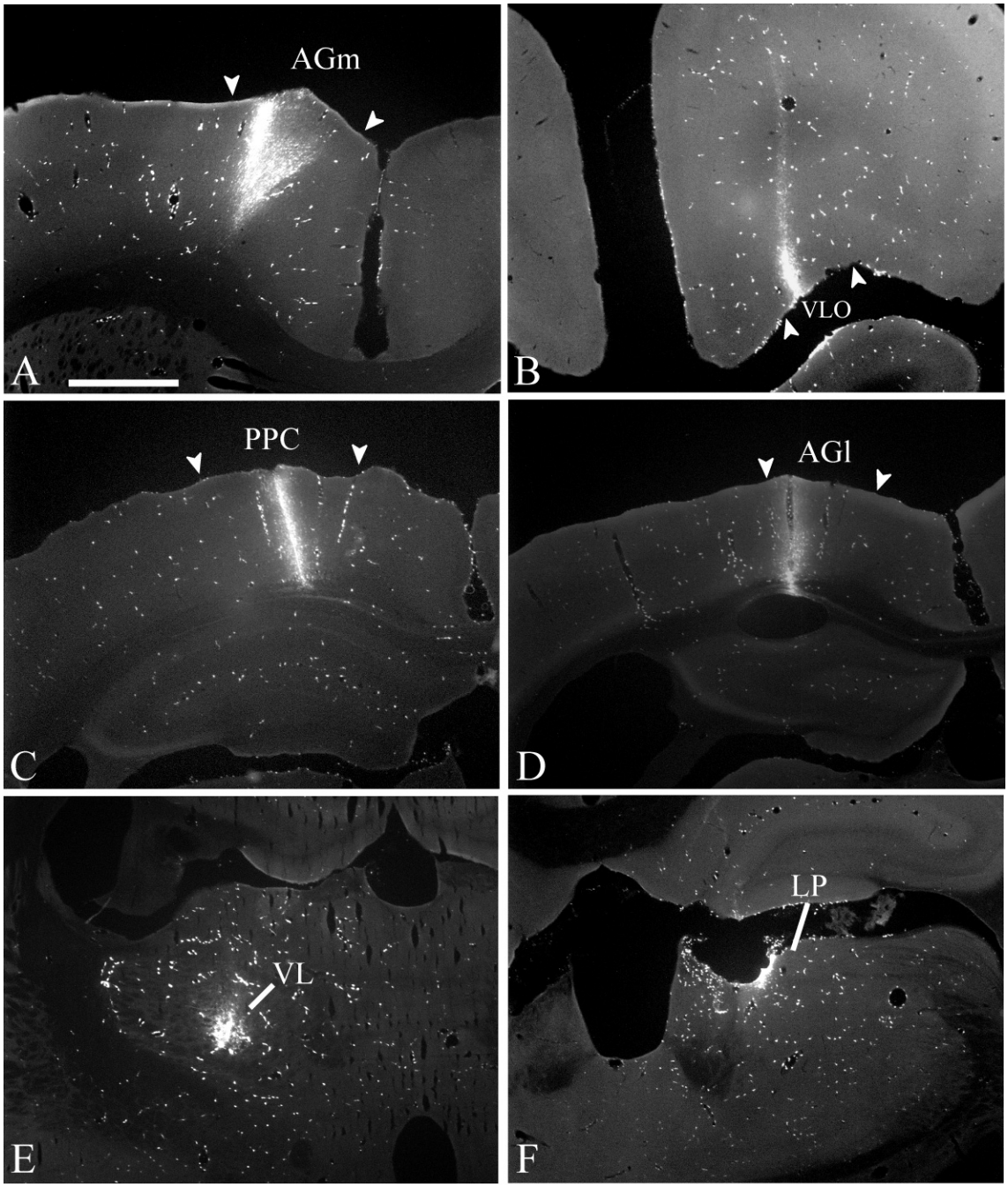

Figure 3-1. Representative fluorescent photomicrographs of cortical and thalamic injection sites. 25x. Scale bar = 1 mm; applies to A-F. A) Injection of AlexaFluor 488 in cortical area AGm (case DCS 178). B) Injection of Fluororuby in cortical area VLO (case DCS 147). C) Injection of Fluororuby in cortical area PPC (case DCS 178). D) Injection of Fluororuby in the caudal portion of cortical area AGl (case DCS 193). E) Injection of Microruby in thalamic nucleus VL (case DCS 173). F) Injection of Microruby in the medial portion of thalamic nucleus LP (case DCS 191).

Injections in AGm/VLO

Case DCS 147 had an AGm injection site centered at a-p +0.7, m-l +1.0, which affected all layers of the cortex without impinging on the white matter. The injection spans a rostrocaudal distance of ~0.3mm. Striatal labeling from this injection was typical of that observed following other AGm injections, and was composed of a densely labeled dorsolateral band and a more diffuse area of labeling in DCS.

The VLO injection site for case DCS 147 was centered at a-p +3.2, m-l +2.2, and d-v -4.2. Terminal fields of axons originating in cortical area VLO were located close to and along the d-v extent of the medial wall in this case (Fig 3-3A). Some labeling produced by the injection extends to border the AGm labeling in DCS from the medial side and interdigitates at the light microscopic level with some of the axons from area AGm, forming a region similar to the focal projection described following PPC injections. In contrast to the PPC focal DCS projection, the discrete region of VLO label remained continuous with the primary field of VLO label along the medial wall. Despite the presence of this seemingly similar focal projection, there was little if any overlap of axons from AGm and VLO evident in this case.

Injections in AGm/VL

Case DCS 173 had an injection centered in rostral AGm (a-p +1.4). The VL injection was centered at a-p -2.5, m-l +1.4, and d-v -6.0, and was limited to nucleus VL (Fig 3-1E). The terminals of axons originating in thalamic region VL were located primarily lateral to DCS. Some terminals were observed dorsolateral to DCS, overlapping with the dorsolateral AGm band, but these were less dense.

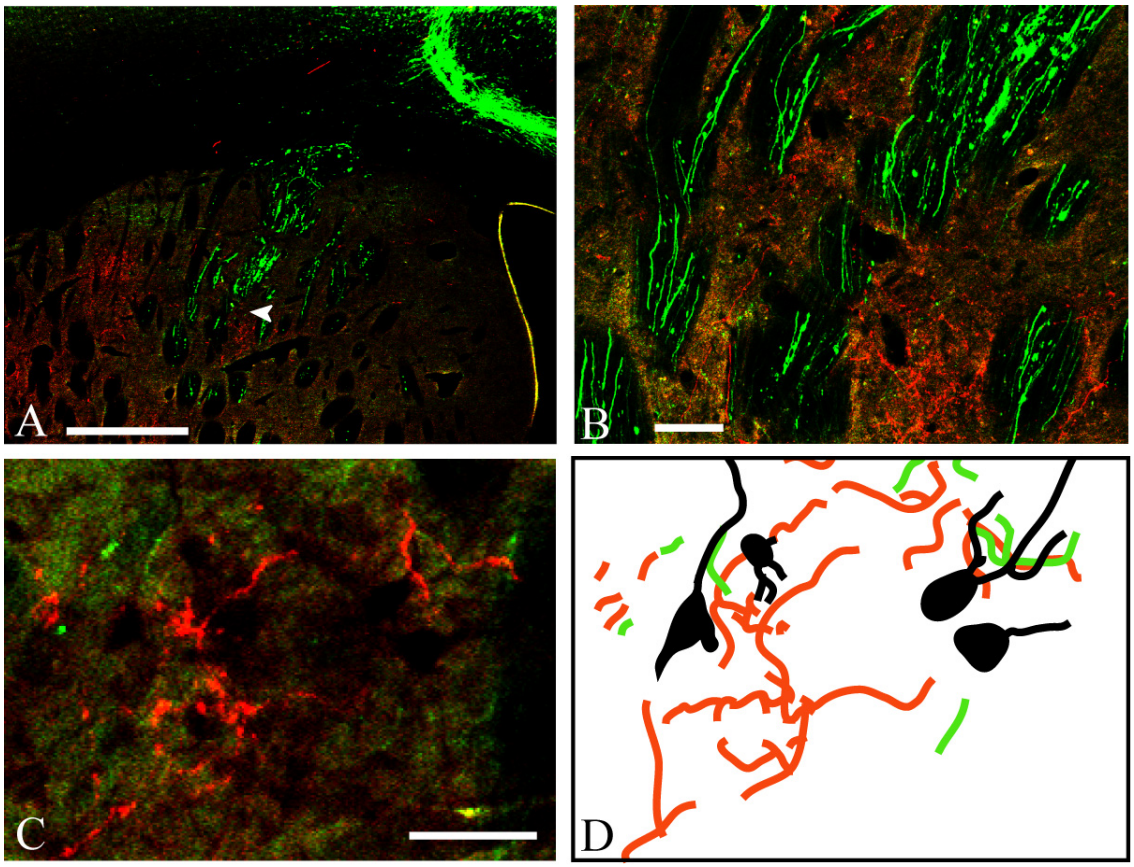

Figure 3-2. Striatal labeling following injection of fluorescent anterograde tracers. A) Labeling following injection in AGm (green) and PPC (red) in case DCS 178. AGm labeling is visible in a green dorsolateral band. Larger-caliber green axons are visible in the white matter fascicles passing through the dorsocentral striatum (DCS). Labeling from the PPC injection also forms a dorsolateral band and terminals are diffusely present in all of DCS. Additionally, a dense focus of labeling is visible in DCS (arrow; B). 50x. Scale bar = 1mm. B) Higher-magnification photomicrograph of the dense focus of labeled PPC axons in case DCS 191. Several AGm axons (green) are visible and cross the PPC axons. The two either touch or pass within 20µm of one another. Larger-caliber green axons are also visible in the white matter fascicles. 100x. Scale bar = 100µm. C) Photomicrograph of axons from cortical areas AGl (green) and PPC (red) in close association with dendritic processes of retrogradely-labeled striatal medium spiny neurons (black) in case DCS 193. 200x. Scale bar = 100µm. D) Line drawing of axons and cell bodies from C.

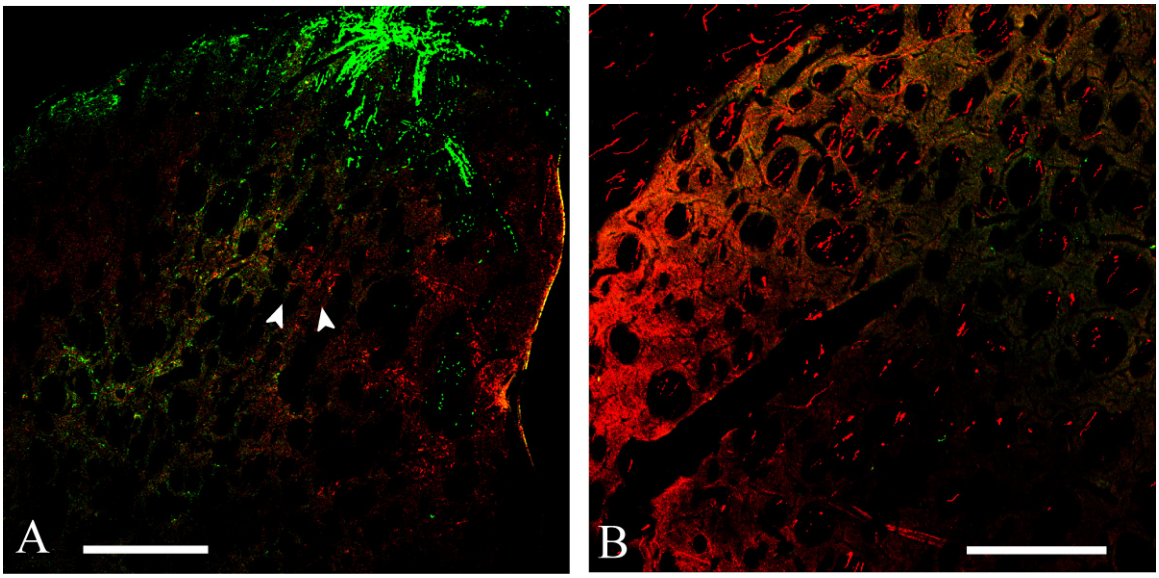

Figure 3-3. Labeling in cases DCS 147 and DCS 173. A) Striatal labeling following injection of fluorescent anterograde tracers in AGm (green) and VLO (red) in case DCS 147. AGm labeling forms a dense green dorsolateral band and a more diffuse region of labeling in the dorsocentral striatum (DCS). Labeling from the VLO injection is most dense along the medial wall, and terminals are diffusely present in all of DCS. Additionally, a dense focus of labeling is visible in or near DCS (arrow), although no overlap was evident between axons from AGm and VLO in the dense focus. 50x. Scale bar = 1 mm. B) Striatal labeling following injection of fluorescent anterograde tracers in cortical area AGm (green) and thalamic nucleus VL (red) in case DCS 173. Labeling from the VL injection is most dense along the lateral edge of the striatum. No terminals were observed in DCS in this case. Large-caliber fibers can be seen passing through the white matter bundles and probably account for VL labeling observed in a previous retrograde study of DCS. 100x. Scale bar = 1 mm.

Heavy fascicular labeling was present throughout much of the rostrocaudal extent of the striatum and was especially dense in and around DCS. Despite the rostral AGm injection, the VL injection in this animal produced striatal labeling that was located rostral to the majority of the observed AGm labeling. There was no overlap between AGm and VL terminal field labeling observed in this case (Fig 3-3B).

Injections in AGm/LP

Case DCS 191 had an AGm injection centered at a-p +1.2 which affected all cortical layers but did not damage the white matter. It is visible on only one section in each spaced series, and therefore had a narrow a-p extent. The MicroRuby injection site in LP was centered at a-p -3.8, m-l +1.3, and d-v -4.5 (Fig 3-1F). The injection site was very focal within medial LP, which resulted in the labeling of a relatively small number of terminal axons in the striatum. However, those that were labeled were very densely filled and easily visualized. The primary terminal field of LP thalamostriatal axons in this case formed a dorsolateral band visually very similar in placement to the one typically seen following injections in cortical area PPC (Fig 3-4A,B,C). Thalamostriatal axons also overlapped diffusely with the dorsolateral AGm band. Within DCS, LP axons extended in long, relatively straight arborizations, which were not observed to this degree or in this conformation following injection in any other cortical area or thalamic nucleus VL (Fig 3-4C,D). These varicosity-dotted long axons overlapped many AGm axons in both the dorsolateral AGm band and within DCS. Axons from LP were evident in the dorsolateral band on both the fluorescent sections and those processed for BDA labeling, but were only visualized effectively in DCS on BDA sections (Fig 3-4).

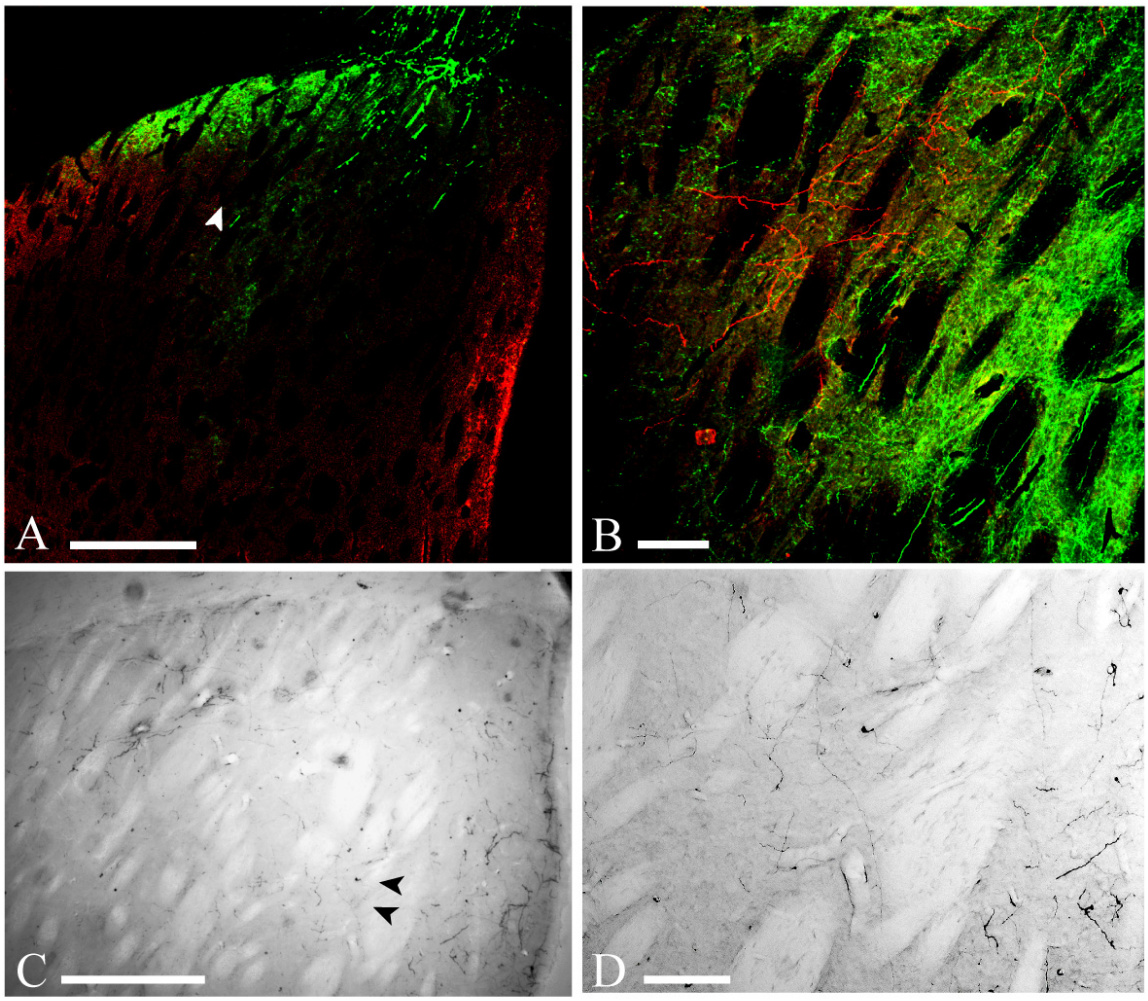

Figure 3-4. Striatal labeling pattern in case DCS 191 following injection of anterograde tracers. A) Fluorescent labeling following injection in cortical area AGm (green) and thalamic nucleus LP (red). Axonal labeling from AGm forms a dense green dorsolateral bandand a more diffuse region of labeling in the dorsocentral striatum (DCS). Labeling from the LP injection also forms a dorsolateral band (arrow; panel B), in which overlap was observed between AGm and LP axons. 50x. Scale bar = 1 mm. B) Axons from thalamic nucleus LP (red) form a band in the dorsolateral striatum and both overlap and interdigitate with axons from cortical area AGm (green). 100x. Scale bar = 100 µm. C) Adjacent section to the one depicted in A and B, processed for BDA (Microruby contains both tetramethylrhodamine and biotin molecules). The dorsolateral band of LP labeling is still evident, and labeling in DCS is more easily visualized. Arrows point to an especially dense focus of axonal labeling in DCS (depicted in D). 62.5x. Scale bar = 1 mm. D) An especially dense focus of labeled axons following injection of Microruby in thalamic nucleus LP. Many axonal varicosities are evident on the labeled axons. 125x. Scale bar = 100 µm.

Injections of BDA in PPC

The brains examined having single injections of BDA in PPC (DCS 60, 77, 88, 91, and 114) each exhibited a pattern of striatal labeling which included a dense focus of axonal terminals located at approximately the level of the anterior commisure (AC), with the exception of DCS 114. Photomicrographs of each PPC focus are presented in Figure 3-5. In all brains with foci, the focus was always located ventromedial to the densest portion of the primary labeling field (band) within a given section. Foci were typically ellipsoid in the a-p dimension, having the largest diameter and greatest density in the approximate center of their anterioposterior extent.

As previously noted, the primary terminal bands of PPC shift in position commensurate with a medial or lateral placement of the BDA injection site [92]. Case DCS 91 had an injection placed in medial PPC (PPCm) and had the most visibly dense focus of axonal labeling (Fig 5A, B). Cases DCS 60, 77, and 114, also had injection sites confined to PPCm. The primary terminal fields and foci in cases 60 and 77 (Fig 5C-5F) resembled those observed in DCS 91, although foci in both brains appeared less dense overall than those in case 91. Case DCS 114 possessed a primary band of label very similar to those seen in 60 and 77, but lacked an observable focus.

Case DCS 88 received a BDA injection in lateral PPC and the primary terminal band was located more dorsolaterally than in the other cases. The focus was also shifted laterally, into the central portion of DCS (Fig 3-5G,H).

In all PPC cases, labeled foci were in the calbindin-positive matrix with few or no axons visible in nearby patch compartments.

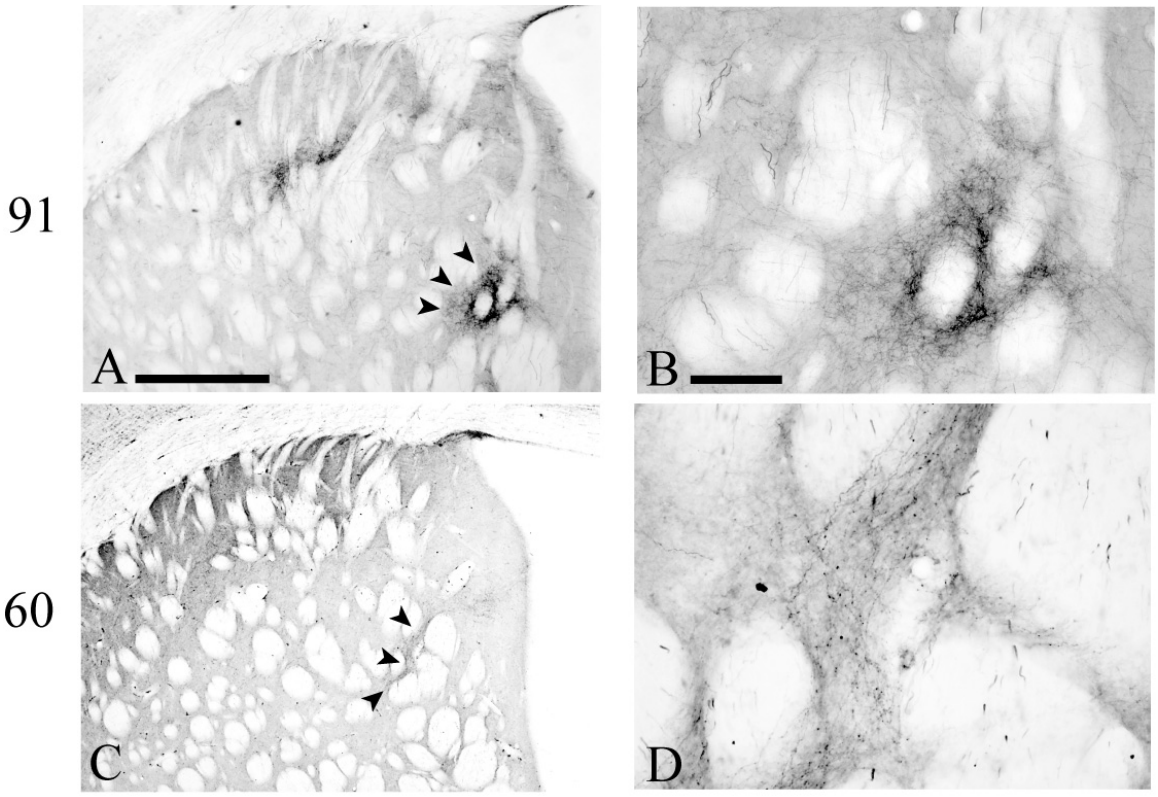

Figure 3-5. Labeled axons in the striatum after injection of BDA in cortical area PPC. In each case there was a dense dorsolateral band of labeling, a diffuse projection to DCS, and a dense focus of labeled axons in DCS. A) Photomicrograph of striatal labeling in case DCS 91. The dense dorsolateral band and dense focus in DCS (arrows) are clearly visible. 62.5x. Scale bar = 1 mm and applies to A, C, E, and G. B) Higher-magnification view of the dense focus of labeled axons in case DCS 91. 125x. Scale bar = 100µm and applies to B, D, F, and H. C) Photomicrograph of striatal labeling in case DCS 60. The dense dorsolateral band and dense focus in DCS (arrows) are clearly visible. D) Higher-magnification view of the dense focus of labeled axons in case DCS 60. E) Photomicrograph of striatal labeling in case DCS 77. The dense dorsolateral band and dense focus in DCS (arrows) are clearly visible. F) Higher-magnification view of the dense focus of labeled axons in case DCS 77. G) Photomicrograph of striatal labeling in case DCS 88. The dense dorsolateral band and dense focus in DCS (arrows) are clearly visible. H) Higher-magnification view of the dense focus of labeled axons in case DCS 88.

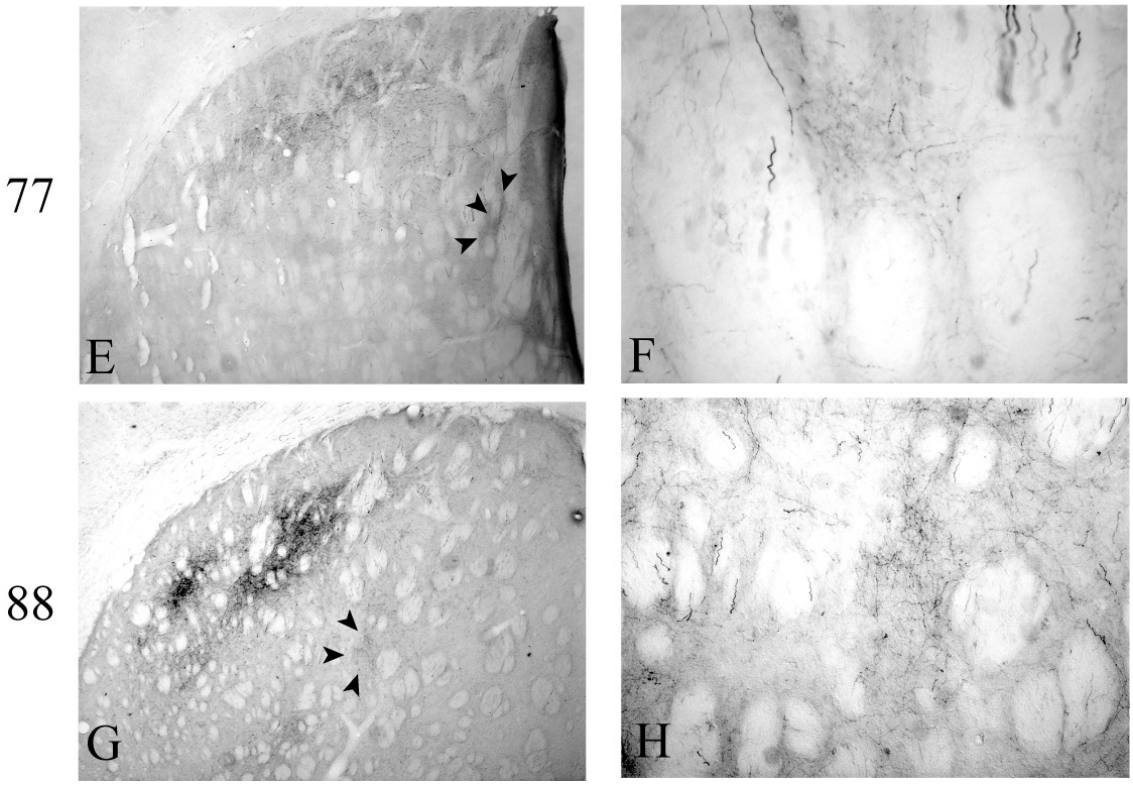

Figure 3-5. Continued

Injections of BDA in Oc2M

Both Oc2M cases examined (DCS 95 and 101) exhibited a focus of labeled axons ventromedial to the primary terminal field. The observed ellipsoid foci qualitatively resembled those seen in PPC brains and were located at or near the level of the AC, as in PPC cases. All observed foci were in the calbindin-positive matrix with few to no axons visible in nearby patch compartments, as in PPC brains.

Other BDA Injections

One brain with a BDA injection in VLO (DCS 110), and another with an AGl injection (DCS 100), had robust labeling in the primary terminal fields (bands), but no foci similar to those seen in PPC or Oc2M brains were observed in either case.

Discussion

One significant finding in my study is that the cortical areas PPC and Oc2M terminate in DCS diffusely and in a focal manner, overlapping and interdigitating with AGm axons, while other cortical areas and thalamic nuclei do not form dense foci of axonal terminals in DCS (cortical areas VLO and AGl and thalamic nuclei LP and VL). Previously, I found that cortical areas AGm, AGl, PPC, VLO, and Oc2M were consistently labeled following injections of a retrograde tracer in and around region DCS (see Chapter 2), and all were observed to form terminal fields near or in DCS in the current anterograde study, and in an earlier report [92]. These areas have all been shown previously to be reciprocally interconnected with one another and with several thalamic nuclei [93].

Fluorescent or BDA injections in AGl did produce the typical dorsolateral band of primary axonal labeling as well as sparse labeling in DCS, but those brains did not exhibit the focal groups of axons in DCS observed following PPC or Oc2M injections.

This is consistent with previous descriptions of AGl labeling [92]. It is demonstrated herein that corticostriatal axons from areas AGm and AGl cross both one another and the dendritic processes of individual retrogradely-filled striatal medium spiny neurons at the light microscopic level. This finding is consistent with the hypothesis that individual medium spiny neurons integrate inputs from multiple cortical and thalamic regions, requiring multiple simultaneous input stimuli to depolarize [17,33,80].

Fluorescent tracer injections in AGm and PPC produced a dorsolateral band of labeled PPC axons between DCS and the dorsolateral AGm band, as well as a discrete focus of labeled PPC axons within AGm. These foci were first described in another AGm/PPC double-fluorescent case [92] and appear to be sites of overlap and interdigitation between axons from AGm and PPC. Herein, the same type of isolated focus of labeled axons was found in an additional double-fluorescent AGm/PPC case (178). Additionally, brains which received single PPC injections of the anterograde tracer BDA were also examined for foci. Four of the five PPC BDA cases exhibit clear foci which are detached from both the primary terminal field (band) and from terminals scattered diffusely throughout DCS. Therefore, it is probable that these foci are a feature common to the PPC/AGm projection and represent a consistent zone of overlap between axons from the two cortical areas.

In a previous report, we described the results of a AGm/Oc2M double-labeling experiment [92]. We demonstrated that Oc2M projects to the striatum in a pattern consistent with the cortical areas examined herein, forming a dense primary area (band) of terminals and a more diffuse secondary area which overlaps partially with labeling

from area AGm in DCS. In the current report, BDA-labeled corticostriatal projections from Oc2M form a focal arborization in DCS similar to those seen in PPC brains.

Small groups of labeled axons similar to those seen following PPC and Oc2M injections were reported by Brown *et. al* following injections of an anterograde tracer into FL and HL [10]. Their presence following injections in both primary somatosensory cortices (FL and HL) and areas involved in secondary and associative tasks (AGm and PPC) suggests that these foci represent a larger-scale pattern of corticostriatal projection.

A visually similar focus of labeling was observed following double labeling of AGm and VLO axons. Although this focus is smaller than the one formed by PPC axons and no overlap was observed, it could also be a zone of overlap on medium spiny neurons located near the interface between AGm and VLO terminal fields. As noted by Wilson [133], the possibility of individual medium spiny neurons integrating information from adjacent yet non-overlapping corticostriatal terminals is a distinct and often overlooked one, due to the size of their dendritic trees. Further, the convergence of axons from non-overlapping corticostriatal projections has been demonstrated electrophysiologically on single medium spiny neurons in the macaque [80]. This may also be true in the rat striatum but it remains to be demonstrated.

It is not surprising that axons from thalamic region VL do not terminate in region DCS, since VL is primarily associated with motor functions, despite the fact that VL was heavily labeled following injections of retrograde tracers in and around DCS. Uptake of retrograde tracers by the large number of labeled axons in the fascicles traveling through DCS is the likely explanation for the VL labeling seen in the previous retrograde study (see Chapter 2). The observed pattern of labeling is consistent with previous anatomical

and electrophysiological data localizing the effects of VL stimulation to lateral striatum [43]. Also, VL is a large nucleus, and the injection did not completely fill it in this case. It is possible that other portions of VL do project to DCS, although the current data suggest that previously reported retrograde labeling of VL was the result of tracer uptake by fibers of passage, as discussed in Chapter 2.

The medial portion of thalamic nucleus LP was found to project densely to a dorsolateral band which overlapped and interdigitated with the primary dorsolateral AGm band, and diffusely to DCS. In Chapter 2, a retrograde study, I reported that LP was labeled only when injections of Fast Blue were placed in DCS itself. Additionally, Erro *et al.* [31] found LP labeling following injection of a retrograde tracer in the dorsal striatum but not in the ventral striatum.

The overlap of corticostriatal terminal fields was noted by Yeterian and Van Hoesen [136]. Many authors have since addressed the topic of overlapping and/or interdigitating corticostriatal terminal fields because of the potent implications. Of particular interest is the overlap in the striatum of efferents from reciprocally interconnected cortical and thalamic areas. In one notable report, a network of reciprocally interconnected cortical and thalamic areas was described in the macaque [74], where interconnected motor-related areas project both to distinct, non-overlapping territories in the basal ganglia, and also project more diffusely to overlapping areas in both the caudate and putamen. Similarly, several groups have demonstrated that forelimb representations from different cortical areas overlap in the macaque putamen [52,111]. This pattern of overlap has also been described in thalamostriatal and corticostriatal projections from rodent somatosensory cortex as well, where there is more convergence

in the striatum from SI areas representing subcomponents of the rodent forelimb than from cortical areas representing noncontiguous body parts [50,51].

In addition to the reports which demonstrated overlap, there are substantial data which suggest that the projections from reciprocally interconnected cortical areas project exclusively to non-overlapping portions of the striatum [104]. One possible explanation for the disparity between the current findings and those of Selemon and Goldman-Rakic is that some cortical areas project in an overlapping way and others in a non-overlapping way, despite their reciprocal interconnection. It is possible that functionally-associated cortical areas (like AGm and PPC) involved in a cortical-subcortical network that relies on the striatum for some integrating function project to the striatum with some degree of overlap depending on the requirements of the specific network, while other cortical areas are entirely segregated. This pattern of selective overlap and segregation was previously reported in the macaque [32].

In my study, as in previous reports, I found that both AGm and PPC form their primary terminal fields as densely labeled bands in dorsolateral striatum which do not overlap [92,93], as reported by Brown *et al*. [10] for rat somatosensory cortex. Also, it is known that areas AGm and PPC project diffusely to region DCS [92]. Herein, I report the existence of a focus of overlap in DCS of projections from AGm and cortical areas PPC and Oc2M. These foci could represent key regions in DCS for multimodal integration of information from AGm with that from PPC and Oc2m. Whether PPC and Oc2M foci overlap with each other in DCS remains an open question and warrants further study. Areas AGm, PPC, and Oc2M all play a critical role in directed attention in the rat. Destruction of DCS, but not dorsolateral striatum, produces robust neglect of

contralesional stimuli which does not spontaneously recover and cannot be relieved by the administration of dopamine agonists [115,116]. The location of these foci within DCS is therefore a significant finding. Axons in the dense foci observed in BDA brains were located in the calbindin-rich matrix compartment. This is consistent with the descriptions of matriosomes in the primate basal ganglia [35] and may indicate an anatomical and functional similarity between the rat foci and primate matriosomes.

It is possible that integration in the diffusely-terminating portion of the rat network mediating directed attention is taking place only on specific subtypes of striatal projection cells, which are typically segregated into patch and matrix groups [55]. It is unlikely, however, that all of the diffuse overlap seen in the striatum is occurring in exclusively patch or matrix compartments. Diffuse overlap is seen at the edge of the AGm/VLO striatal terminal fields and LP neurons extend relatively long distances in the dorsolateral AGm band as well as in DCS, forming many distinct en passant type axonal varicosities. In a previous paper, we reported that the majority of labeled axons in DCS were in the matrix compartment following cortical placement of BDA [92]. It is likely, therefore, that the majority of the diffuse overlap observed in multiple-labeled cases is occurring in the matrix compartment.

CHAPTER 4
PHOTOTHROMBOTIC LESION OF POSTERIOR PARIETAL CORTEX IN THE RAT

Introduction

The rat model of hemispatial neglect has yielded key information regarding the role of the medial agranular cortex (AGm) and the posterior parietal cortex (PPC) in a cortico-striato-thalamic network mediating directed attention [16,18,92]. An aspiration lesion of either area AGm or area PPC results in a lasting neglect of contralesional hemispace, similar to that seen following unilateral PPC damage in humans [11,16,115,117]. In rats, symptoms of neglect do not spontaneously recover over time. This is also consistent with the human syndrome, in which 25% of patients still show reduced spatial capacity after 12 years, often after attempting physical therapy [57].

In previous experiments, lesions were produced by removing either AGm or PPC via aspiration [14,116]. While aspiration lesions effectively produce neglect, the ability to induce a more physiologically-relevant lesion would represent an improvement for the rat neglect model in several ways. First, a craniotomy is required to reach the surgical site for an aspiration lesion. During this procedure, the bone and meninges immediately external to the cortical area of interest are removed by the surgeon. Tampering with these tissues is undesirable because of the increased risk of secondary complications related to bone or meningial trauma. The dorsal saggital sinus is also placed at risk during this procedure, presenting the chance that a subject could experience uncontrollable bleeding during the aspiration lesion.

Second, an aspiration lesion risks damaging the white matter forming the cingulum bundle, which is located internal to AGm. Damage to the cingulum bundle could result in inappropriate behavior changes in addition to those expected from the intended lesion and may interfere with sprouting from contralesional cortex, if occurring. Third, acute removal of brain tissue most likely does not result in the replication of the cell signal cascades produced in response to a focal ischemic attack, since the cells are not undergoing necrosis or apoptosis in situ. Also, spreading depression-like effects may be artificially minimized by an aspiration lesion. Due to the disruption in cell signaling, cortical remodeling (as measured by changes in GAP-43 expression), and functional recovery from behavioral or motor deficits are likely adversely affected following aspiration [81,110,112].

For these reasons, I explored the practicality of making a photothrombotic lesion limited to the cortical area of interest, without performing a craniotomy, leaving the tissues in place to more closely replicate the physiological state of the brain post-infarct. This procedure relies on the unique qualities of an injectable dye, Erythrosin B, which is placed in the venous system. When light of a known wavelength and intensity strikes the molecules of the dye in the blood, a series of events is initiated which results in the formation of a thrombus localized to the area struck by the light (PPC in this case). Photothrombosis relies on the natural process of thrombogenesis following a vascular insult. In the case of Erythrosin-B mediated photothrombosis, the insult is in the form of photochemically-mediated peroxidation of the lipids in the membranes of cells forming the vascular endothelium. This vascular damage is caused by the donation of valence electrons from the dye molecules to the endothelial cells and results in platelet adhesion

and aggregation, which result in the formation of a vascular occlusion (thrombus) [125]. The highest level of platelet aggregation occurs at the pial surface since it is exposed to the most direct light. It is possible to monitor the progression of the lesion via nuclear magnetic resonance imaging, and multiple MRI studies have plotted the time course of photothrombotic lesions under different parameters [68,70,88,113,123].

Materials and Methods

A total of 24 male Long-Evans Hooded rats were used in my study. Rats were anesthetized with a Ketamine/xylazine cocktail (87:13 mixture; 80 mg/Kg, ip). The head was shaved and ointment put in the eyes to prevent drying during surgery. Upon exhibiting no eyeblink response or withdrawal to ear bar placement, anesthetized rats were fixed in a stereotaxic apparatus and the skull exposed. A drop of mineral oil was placed on the skull to render the surface optically smooth. Either rose bengal or erythrosin-B (20mg/mL in PBS; 20mg/kg; RB:Sigma 3300000; EB:Sigma 200964) were injected into the medial saphenous vein or the tail vein. The maximum absorbance for rose bengal and erythrosin-b are 549nm and 533nm, respectively, but both are effective when excited at 532nm [125]. Immediately following the dye injection, the brain was transcranially illuminated via either a Schott light source (KL2500-LCD) with a custom filter limiting the transmitted light to a 50nm band centered on 532nm (Omega Optical) or a frequency-doubled YAG-laser with output at 532 nm and power ~100 mW (250 mW/cm^2; LAGR100; Information Unlimited) for a maximum of 8 minutes, after which time the dye concentration in the blood stream is below that necessary to cause a thrombus. Following the illumination period, an antibiotic ointment was placed between the skin and the skull, and the incision was closed with wound clips. After a survival period of five to ten days, rats were injected IP with a barbiturate solution (Beuthanasia-

D; 100mg/kg IP) and perfused intracardially with 300 mL of phosphate buffered saline (PBS) followed by 300 mL of 4% buffered paraformaldehyde. Brains were subsequently removed and cryoprotected by incubation in a 30% sucrose solution. Coronal sections were cut on a freezing microtome at 40μm and placed in dilute fixative until being mounted on slides. Cresyl violet staining was performed for cytoarchitectural analysis and description of the lesion site.

Results and Discussion

The lesion was much more difficult to make than expected. Many papers misrepresent the difficulty of the procedure, often as the result of the use of flawed methodology [59,88,103,129]. In one report, researchers injected Rose Bengal into the femoral vein in an uncontrolled fashion, sometimes used immense doses (as much as 80mg/kg), illuminated for a much longer amount of time than their dye molecule of choice could actually be present in the bloodstream, and irradiated via an unfiltered "cold light source" [129]. In one murine model, authors injected the dye intraperitoneally at a low dose (10mg/kg), waited five minutes, and irradiated with an unfiltered light source for 15 minutes, which is much longer than the time in which rose bengal is at an active concentration following injection [103]. Similarly, researchers designing a rat model of photothrombotic infarct in epileptic rats expose the brain to unfiltered light (400 nm to 1200 nm) for 20 minutes [59]. Another group irradiated for 30 minutes [88], which is similarly well past the eight minutes it takes for the rat liver to remove rose bengal from the blood stream [126,127].

In all of the above cases, the investigators exposed the brain to unnecessary wavelengths of light, which are not absorbed by the dye molecules, used an unnecessary period of illumination to induce infarcts, and did not perform controls to ensure there

were no burns produced by the light source. There is no such thing as a "cold light source" [70]. Excess light energy does not simply disappear, in accordance with the law of conservation of energy. In this case, unabsorbed light is converted to heat energy, which does an unknown amount of tissue damage separate from that caused by the photo-excited dye molecules [70].

With the aim of controlling these errors, I began my trials with a Schott light source and a filter from Omega Optical, which limited the wavelength of the transmitted light to a 30 nm band centered on 530 nm. Only light capable of exciting the RB in the brain was emitted while using this apparatus, which greatly limited the chance of causing heat-related damage. Conversely, a thermometer placed against the surface of the fiber optic gooseneck on the Schott quickly rose 10 to 15°C without the filter in place to restrict the spectra emitted by the "cool light source." When the Omega filter (green) was placed in the light path, this temperature rise was eliminated. Control animals which received filtered irradiation alone (no dye) did not have heat lesions.

I was able to make lesions reasonably consistently using the green Omega filter and the Schott light source, but the lesions were very large (Fig 4-1). It is possible to limit the size of the lesions by using an optically opaque substance (i.e. a brass shim) to protect the non-target portions of the skull and the underlying brain regions from the light source. Unfortunately, lesions produced with the Schott/Omega are somewhat variable depending on the distance of the light source from the skull, since the light emitted from the fiber optic gooseneck spreads rapidly. This spread results in reduced power with distance.

For roughly the same price as the Schott/Omega setup, I purchased a frequency-doubled YAG-laser with output at 532 nm and power ~100 mW (250 mW/cm^2;

LAGR100; Information Unlimited). The laser provides several immediate benefits over the Schott/Omega setup. First, the laser does not produce energy capable of causing heat damage to the brain. Second, the beam of laser energy does not spread rapidly and therefore produces lesions which are much more reproducible between animals.

Several factors affected the decision regarding an appropriate injection site for the dye molecule in the rat model of hemispatial neglect. Many researchers inject their dye of choice into the femoral vein, including those who developed the initial protocols [125]. However, gaining access to the femoral vein requires cutting a muscle and is painful for the animal post-surgery. Since any post-surgical pain could interfere with locomotion, which is frequently measured in behavioral testing, a deficit resulting from the surgery would represent a significant confound in nearly any behavioral test and is highly undesirable.

Therefore, I wanted to design a methodology that would interfere minimally with behavioral testing. First, I tried using the lateral tail vein. The lateral tail vein is frequently chosen as a venous access in rats due to its relative availability [47]. Trials with the lateral tail vein were largely unsuccessful. In albino rat strains, the lateral tail vein is relatively easy to visualize and inject, since their tails are a pale pink color and the vein is red. Long-Evans Hooded rats, the strain used in the Corwin/Reep model as well as in many behavioral models, have a heavily pigmented tail, and visualization of the lateral tail vein is very difficult. Since the vein is so small, placing a needle in it is extremely difficult without visualizing the vein.

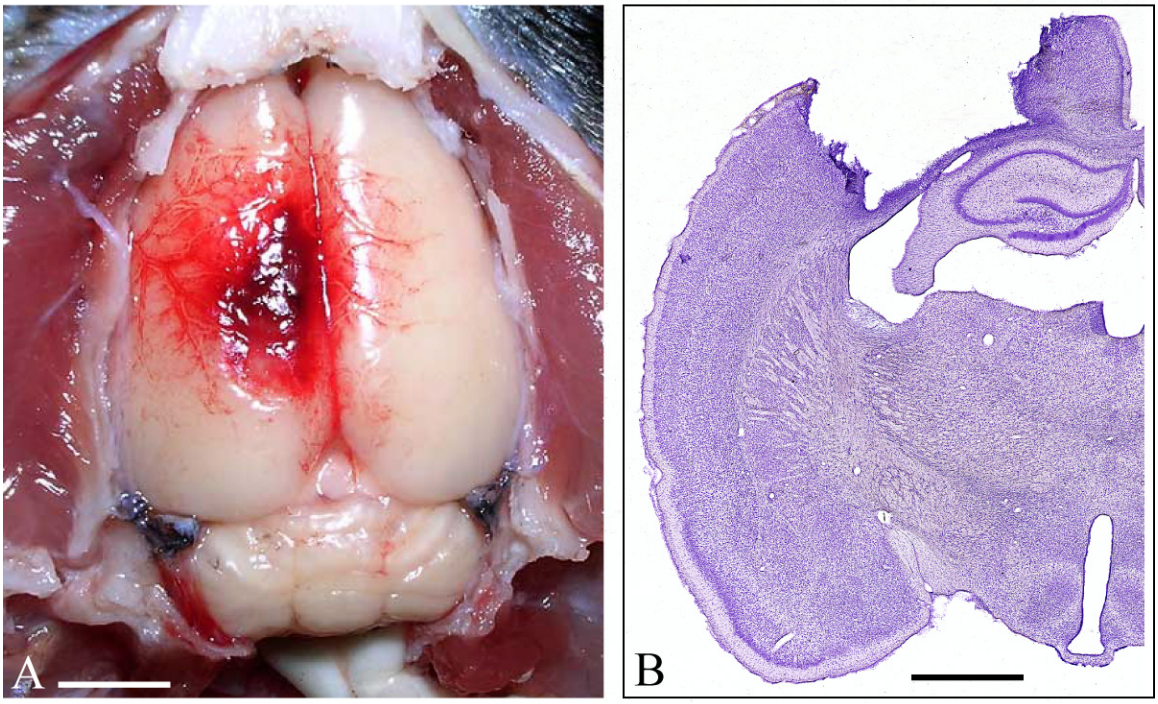

Figure 4-1. Lesion produced via irradiation with the Schott/Omega filter combination. A) Gross lesion at seven days post-photothrombosis. B) Cresyl violet section through the center of the lesion. The lesion is deep and affects the white matter. Note that the medial cortical areas are intact due to the blood supply from the anterior cerebral artery (ACA), which is not affected by the photothrombotic lesion of cortical areas supplied by the branches of the middle cerebral artery (MCA).

If either Rose Bengal or Erythrosin-B is placed outside the vein, a thrombus will not develop in the brain after irradiation, and there is a good chance of necrosis of the tail distal to the injection site. This complication is obviously undesirable. For this reason, I examined other venous routes.

After consulting an anatomy text [47], I decided on the medial saphenous vein, a branch of the femoral vein. The medial saphenous vein is located on the medial side of each hindlimb and is best visualized transdermally after shaving the medial hindlimb. Since the injected volume is usually ~0.5 mL, I found it easiest to use a 1 mL insulin syringe with an attached 27-gauge needle.

One benefit of photothrombosis is that the size of the lesion can be easily controlled. It is simple, for example, to make a large lesion with the filtered Schott light source, since the aperture of the Schott's fiber optic gooseneck is 4 mm. The laser beam is only 2 mm diameter, which makes it useful for more precise lesions (Figure 4-2). It is possible to reduce the size of the lesion resulting from the Schott light source if an opaque substance is placed over the portions of the skull directly over brain regions which are to be spared [22,24-27,126,127].

I began this project with rose bengal, the photoreactive dye most commonly used in the literature [22-28,126-128]. The use of rose bengal is complicated by one major physiological complication: infusion of the dye over any period shorter than 90 seconds produces dangerous fluctuations in the animal's blood pressure [125]. This fluctuation does not occur after infusion of the photoreactive dye erythrosin-b [125] and it was chosen because of this property. This lesion works well in PPC and reliably produces a circular lesion with a ~2mm diameter.

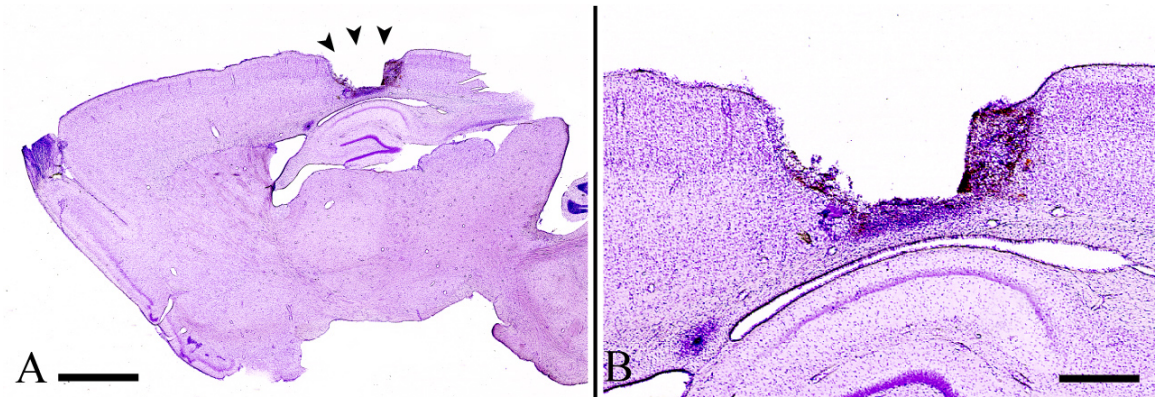

Figure 4-2. Lesion produced via irradiation with the YAG laser. A) Cresyl violet section through the center of the lesion at 21 days post-photothrombosis (saggital view). Scale bar = 2 mm. B) Higher magnification view of the lesion site. The lesion is deep but does not appear to affect the white matter. Scale bar = 0.5 mm.

The lesion affects all layers of the cortex but appears to stop external to the white matter. Conversely, I have not successfully created a lesion of AGm via photothrombosis.

This failure is probably due to the protection of AGm by the dorsal sagittal sinus (which may prevent transmitted laser energy from reaching the cortex), the inability to effectively occlude branches of the anterior cerebral artery supplying AGm, or some combination of the two. If photothrombosis is to be used to study the Corwin/Reep model of directed attention, it will most likely be necessary to study the attentional effects of a PPC lesion instead of an AGm lesion. Despite this change, the directed attention model could be improved overall by the use of a carefully controlled photothrombotic lesion instead of an aspiration lesion, because of the lesion's similarities to occlusive stroke.

CHAPTER 5
CONCLUSIONS AND FUTURE DIRECTIONS

The work described herein began as a retrograde study of afferents to DCS. That study, presented in Chapter 2, used the retrograde tracers Fast Blue and Diamidino Yellow to determine which cortical areas and thalamic nuclei project to the dorsocentral striatum (DCS) in the rat. Retrograde tracers were placed in DCS where they were subsequently absorbed by axon terminals and transported retrogradely to the cell bodies of origin. I then observed which cortical areas and thalamic regions possessed fluorescent-labeled cell bodies and therefore sent axonal projections to DCS.

The retrograde study revealed that most cortical areas project to some portion of DCS or an adjacent striatal region. Most cortical areas were only labeled in some cases, but AGm, PPC, and Oc2M, the cortical areas known to be part of the network mediating directed attention in the rat, possessed retrogradely-labeled cell bodies in every case.

One inherent problem with studies employing retrograde tracers is the potential for tracer-uptake by axons which are not actually making synapses in the area of interest, but are rather simply passing through the area. This potential necessitates that anterograde studies, where tracers are transported from the cell body toward axon terminals, be carried out. We published data from a study in which we injected rats with biotinylated dextran amine (BDA) and examined the terminal fields of individual cortical areas [92], which allowed the production of a general schematic of potential overlap and interdigitation of cortical inputs to DCS. Additionally, we published double-labelling observations from one AGm/PPC and one AGm/Oc2M brain in the same paper [92]. The

larger double-anterograde study presented in Chapter 3 goes much further, detailing the overlap and interdigitation of AGm with cortical areas PPC, Oc2M, and VLO, as well as with thalamic regions LP and VL. Additionally, Chapter 3 adds descriptions of previously undescribed dense foci of axonal labeling in DCS following placement of an anterograde tracer in either PPC or Oc2M, but not VLO. These dense matriosome-like foci are sites of increased overlap between axons from cortical areas PPC and Oc2M with axons from AGm. The observed foci may therefore represent key sites of integration of multimodal spatial information from these anatomically non-adjacent cortical areas. Importantly, these foci were observed in every brain with an anterograde tracer injection placed in Oc2M, and every brain except one following PPC injection. Therefore, the presence of dense foci within DCS appears to be an anatomical pattern and not just an anomaly. It would be interesting to double-label PPC and Oc2M to determine if their individual dense DCS foci overlap and/or interdigitate with one another. In addition, electron-microscopic studies could be performed to further examine the degree to which axonal projections from cortical areas AGm, PPC, and Oc2M, and thalamic nucleus LP, form synapses with the same individual medium spiny neurons in DCS.

The anatomical studies presented in Chapters 2 and 3 enhanced the previous knowledge of the connections of the cortical and subcortical portions of the network mediating direct attention in the rat. When taken together with the past studies discussed in Chapter 1 [12,16,92,93,95,96], one can build a more detailed picture of the anatomical connections of this network, which subsequently allows the formation of hypotheses regarding the functional aspects of the anatomical network.

The basic anatomy of the system is not extremely complicated. First, it is commonly accepted that sensory information from all modalities enters the brain at the level of the sensory thalamus, which sends projections to primary sensory cortices. The primary sensory areas project to secondary and associative cortices, all of which in turn project to motor cortices, to the sensory thalamic nuclei, and to the striatum. Cortical motor areas project to the motor thalamus, to the striatum, to brainstem targets, and directly into the corticospinal tract. The striatum receives glutamatergic inputs from all of these cortical regions and thalamic nuclei, limbic cortical regions, and also receives dopaminergic inputs from substantia nigra. The only efferent targets of DCS are the substantia nigra and globus pallidus, both of which project to the motor thalamus. The findings presented herein are consistent with these general patterns and extend our knowledge regarding how cortical and thalamic striatal afferents relate to one another and to medium spiny neurons in DCS. DCS appears to be the place where signals from all of these diverse brain structures are integrated, leading to the successful functioning of a mechanism for directing attention toward salient objects in space. The myriad interactions between neurotransmitters, receptors, and the implications for combining information from these diverse regions are far from being understood and add several levels of further complexity to understand when forming hypotheses about the precise functioning of this anatomical network mediating a behavioral process. It is known that striatal medium spiny neurons require synchronous, convergent input from multiple neurons in order to depolarize [131,133], and it is very possible that the corticostriatal projections outlined herein are interacting at some level, but this remains to be demonstrated. To move beyond the current limited understanding of the functioning of

this network, electrophysiological studies are necessary. It is important to define the mechanism by which corticostriatal inputs are synchronized. This synchrony could be the result of interhemispheric corticocortical coupling of contralateral homotopic cortical areas and this has been hypothesized, but remains unknown [133]. The authors of one recent paper which studied the function of neurons in DCS found that striatal neurons which fire in response to spatial information and those which fire in response to rewards are different populations [102].

Now is the time to ask how far to go toward an understanding of the function of the network itself, on a small scale. The main goal of this model's development is to develop potential therapeutics for human patients, which is something that a deeper understanding of the actual computational functioning of the network itself may or may not actually aid. The Corwin/Reep model may well have reached the point now where future studies should be aimed at increasing the degree of functional recovery following a neglect-inducing event (stroke, trauma, etc.). The current lesion model is undesirable for pursuing functional recovery of neglect following stroke, which is the most common cause of neglect in humans, as discussed in Chapter 4.

Photothrombotic lesions are a good alternative for studies of functional recovery from neglect because they replicate a stroke much more closely than does an aspiration lesion [125], while still allowing the production of a lesion which is limited to one anatomical region, which is vital to interpreting experimental outcomes.

LIST OF REFERENCES

[1] G.E. Alexander, M.D. Crutcher and M.R. DeLong, Basal ganglia-thalamocortical circuits: Parallel substrates for motor, oculomotor, "prefrontal" and "limbic" functions, *Prog Brain Res*, 85 (1990) 119-146.

[2] G.E. Alexander, M.R. DeLong and P.L. Strick, Parallel organization of functionally segregated circuits linking basal ganglia and cortex, *Annu Rev Neurosci*, 9 (1986) 357-381.

[3] K.D. Alloway, J. Crier, J.J. Mutic and S.A. Roy, Corticostriatal projections from rat barrel cortrex have an anisotropic organization that correlates with vibrissal whisking behavior, *J Neurosci*, 19 (1999) 10908-10922.

[4] K.D. Alloway, J.J. Mutic and J.E. Hoover, Divergent corticostriatal projections from a single cortical column in the somatosensory cortex of rats, *Brain Res*, 785 (1998) 341-346.

[5] R.M. Beckstead, An autoradiographic examination of corticocortical and subcortical projections of the mediodorsal-projection (prefrontal) cortex in the rat, *J Comp Neurol*, 184 (1979) 43-62.

[6] H.W. Berendse, Y. Galis-de Graaf and H.J. Groenewegen, Topographical organization and relationship with ventral striatal compartments of prefrontal corticostriatal projections in the rat, *J Comp Neurol*, 316 (1992) 314-347.

[7] H.W. Berendse and H.J. Groenewegen, Organization of the thalamostriatal projections in the rat, with special emphasis on the ventral striatum, *J Comp Neurol*, 299 (1990) 187-228.

[8] H.W. Berendse and H.J. Groenewegen, Restricted cortical termination fields of the midline and intralaminar thalamic nuclei in the rat, *Neuroscience*, 42 (1991) 73-102.

[9] J.J. Bouyer, D.H. Park, T.H. Joh and V.M. Pickel, Chemical and structural analysis of the relation between cortical inputs and tyrosine hydroxylase-containing terminals in rat neostriatum., *Brain Res*, 302 (1984) 267-75.

[10] L.L. Brown, D.M. Smith and L.M. Goldbloom, Organizing principles of cortical integration in the rat neostriatum: Corticostriate map of the body surface is an ordered lattice of curved laminae and radial points, *J Comp Neurol*, 392 (1998) 468-488.

[11] K.J. Burcham, J.V. Corwin, M.L. Stoll and R.L. Reep, Disconnection of medial agranular and posterior parietal cortex produces multimodal neglect in rats, *Behav Brain Res*, 86 (1997) 41-7.

[12] H.C. Chandler, V. King, J.V. Corwin and R.L. Reep, Thalamocortical connections of rat posterior parietal cortex, *Neurosci Lett*, 143 (1992) 237-42.

[13] F. Conde, Further studies on the use of the fluorescent tracers fast blue and diamidino yellow: Effective uptake area and cellular storage sites, *J Neurosci Methods*, 21 (1987) 31-43.

[14] J. Corwin, K. Burcham and G. Hix, Apomorphine produces an acute dose-dependent therapeutic effect on neglect produced by unilateral destruction of the posterior parietal cortex in rats., *Behav Brain Res*, 79 (1996) 41-9.

[15] J.V. Corwin, S. Kanter, R.T. Watson, K.M. Heilman, E. Valenstein and A. Hashimoto, Apomorphine has a therapeutic effect on neglect produced by unilateral dorsomedial prefrontal cortex lesions in rats, *Exp Neurol*, 94 (1986) 683-698.

[16] J.V. Corwin and R.L. Reep, Rodent posterior parietal cortex as a component of a cortical network mediating directed spatial attention, *Psychobiology*, 26 (1998) 87-102.

[17] R.L. Cowan and C.J. Wilson, Spontaneous firing patterns and axonal projections of single corticostriatal neurons in the rat medial agranular cortex, *J Neurophysiol*, 71 (1994) 17-32.

[18] D.P. Crowne and M.N. Pathria, Some attentional effects of unilateral frontal lesions in the rat, *Behav Brain Res*, 6 (1982) 25-39.

[19] D.P. Crowne, C.M. Richardson and G. Ward, Brief deprivation of vision after unilateral lesions of the frontal eye field prevents contralateral inattention, *Science*, 220 (1983) 527-530.

[20] M. Delong, The Basal Ganglia. In E. Kandel, J. Schwartz and T. Jessell (Eds.), *Principles of Neuroscience*, McGraw-Hill, NY, 2000.

[21] M. Deschenes, J. Bourassa and A. Parent, Striatal and cortical projections of single neurons from the central lateral thalamic nucleus in the rat, *Neuroscience*, 72 (1996) 679-687.

[22] W.D. Dietrich, R. Busto, B.D. Watson, P. Scheinberg and M.D. Ginsberg, Photochemically induced cerebral infarction 2: Edema and blood-brain-barrier disruption, *Acta Neuropathol (Berl)*, 72 (1987) 326-334.

[23] W.D. Dietrich, Z.C. Feng, H. Leistra, B.D. Watson and M. Rosenthal, Photothrombotic infarction triggers multiple episodes of cortical spreading depression in distant brain regions, *J Cereb Blood Flow Metab*, 14 (1994) 20-8.

[24] W.D. Dietrich, M.D. Ginsberg, R. Busto and B.D. Watson, Photochemically induced cortical infarction in the rat 1: Time course of hemodynamic consequences, *J Cereb Blood Flow Metab*, 6 (1986) 184-194.

[25] W.D. Dietrich, M.D. Ginsberg, R. Busto and B.D. Watson, Photochemically induced cortical infarction in the rat 2: Acute and subacute alterations in local glucose-utilization, *J Cereb Blood Flow Metab*, 6 (1986) 195-202.

[26] W.D. Dietrich, B.D. Watson, R. Busto, M.D. Ginsberg and J.R. Bethea, Photochemically induced cerebral infarction 1: Early microvascular alterations, *Acta Neuropathol (Berl)*, 72 (1987) 315-325.

[27] W.D. Dietrich, B.D. Watson, R. Busto, P. Scheinberg and M.D. Ginsberg, Photochemically induced microvascular injury - Local and remote consequences, *Ann Neurol*, 20 (1986) 160-160.

[28] W.D. Dietrich, B.D. Watson, M. Wachtel, R. Busto and M.D. Ginsberg, Ultrastructural analysis of photochemically induced thrombotic stroke in rat-brain, *Stroke*, 15 (1984) 191-191.

[29] J. Donoghue and M. Herkenham, Neostriatal projections from individual cortical fields conform to histochemically distinct striatal compartments in the rat., *Brain Res*, 365 (1986) 397-403.

[30] A. Ebrahimi, R. Pochet and M. Roger, Topographical organization of the projections from physiologically identified areas of the motor cortex to the striatum in the rat, *Neurosci Res*, 14 (1992) 39-60.

[31] M.E. Erro, J.L. Lanciego and J.M. Gimenez-Amaya, Re-examination of the thalamostriatal projections in the rat with retrograde tracers, *Neurosci Res*, 42 (2002) 45-55.

[32] A.T. Ferry, D. Ongur, X.H. An and J.L. Price, Prefrontal cortical projections to the striatum in macaque monkeys: Evidence for an organization related to prefrontal networks, *J Comp Neurol*, 425 (2000) 447-470.

[33] D.M. Finch, Neurophysiology of converging synaptic inputs from the rat prefrontal cortex, amygdala, midline thalamus, and hippocampal formation onto single neurons of the caudate/putamen and nucleus accumbens, *Hippocampus*, 6 (1996) 495-512.

[34] A.W. Flaherty and A.M. Graybiel, Corticostriatal transformations in the primate somatosensory system. Projections from physiologically mapped body-part representations, *J Neurophysiol*, 66 (1991) 1249-63.

[35] A.W. Flaherty and A.M. Graybiel, Two input systems for body representations in the primate striatal matrix: experimental evidence in the squirrel monkey, *J Neurosci*, 13 (1993) 1120-37.

[36] A.W. Flaherty and A.M. Graybiel, Input-output organization of the sensorimotor striatum in the squirrel-monkey, *J Neurosci*, 14 (1994) 599-610.

[37] C.R. Gerfen, The neostriatal mosaic: Compartmentalization of corticostriatal input and striatonigral output systems, *Nature*, 311 (1984) 461-4.

[38] C.R. Gerfen, The neostriatal mosaic I: Compartmental organization of projections from the striatum to the substantia nigra in the rat, *J Comp Neurol*, 236 (1985) 454-76.

[39] C.R. Gerfen, The neostriatal mosaic: striatal patch-matrix organization is related to cortical lamination, *Science*, 246 (1989) 385-8.

[40] C.R. Gerfen, The neostriatal mosaic: multiple levels of compartmental organization, *J Neural Transm Suppl*, 36 (1992) 43-59.

[41] C.R. Gerfen, Molecular effects of dopamine on striatal-projection pathways, *Trends Neurosci*, 23 (2000) S64-70.

[42] P. Glees, The anatomical basis of cortico-striate connections., *J Anat*, 78 (1944) 47-51.

[43] G. Glynn and S.O. Ahmad, Three-dimensional electrophysiological topography of the rat corticostriatal system, *J Comp Physiol A Neuroethol Sens Neural Behav Physiol*, 188 (2002) 695-703.

[44] P.S. Goldman and W.J. Nauta, An intricately patterned prefronto-caudate projection in the rhesus monkey, *J Comp Neurol*, 72 (1977) 369-86.

[45] A.M. Graybiel, T. Aosaki, A.W. Flaherty and M. Kimura, The basal ganglia and adaptive motor control, *Science*, 265 (1994) 1826-1831.

[46] H.J. Groenewegen, H.W. Berendse, J.G. Wolters and A.H. Lohman, The anatomical relationship of the prefrontal cortex with the striatopallidal system, the thalamus and the amygdala: evidence for a parallel organization, *Prog Brain Res,* 85 (1990) 95-116; discussion 116-118.

[47] R. Hebel and M.W. Stromberg, *Anatomy of the laboratory rat*, Williams & Wilkins, Baltimore, 1976.

[48] K.M. Heilman, R.T. Watson and E. Valenstein, Neglect and related disorders, *Clinical Neuropsychology (3rd ed.)* (1993) 279-336.

[49] R.R. Hicks and M.F. Huerta, Differential thalamic connectivity of rostral and caudal parts of cortical area Fr2 in rats, *Brain Res*, 568 (1991) 325-329.

[50] Z.S. Hoffer and K.D. Alloway, Organization of corticostriatal projections from the vibrissal representations in the primary motor and somatosensory cortical areas of rodents, *J Comp Neurol*, 439 (2001) 87-103.

[51] J.E. Hoover, Z.S. Hoffer and K.D. Alloway, Projections from primary somatosensory cortex to the neostriatum: the role of somatotopic continuity in corticostriatal convergence, *J Neurophysiol*, 89 (2003) 1576-87.

[52] M. Inase, S.T. Sakai and J. Tanji, Overlapping corticostriatal projections from the supplementary motor area and the primary motor cortex in the macaque monkey: An anterograde double labeling study, *J Comp Neurol*, 373 (1996) 283-296.

[53] E.G. Jones, *The thalamus*, Plenum Press, New York, 1985, xvii, 935 p. pp.

[54] E.G. Jones, J.D. Coulter, H. Burton and R. Porter, Cells of origin and terminal distribution of corticostriatal fibers arising in sensory-motor cortex of monkeys, *J Comp Neurol*, 173 (1977) 53-80.

[55] Y. Kawaguchi, Neostriatal cell subtypes and their functional roles, *Neurosci Res*, 27 (1997) 1-8.

[56] J.M. Kemp and T.P. Powell, The cortico-striate projection in the monkey, *Brain*, 93 (1970) 525-46.

[57] G. Kerkhoff, Spatial hemineglect in humans, *Prog Neurobiol*, 63 (2001) 1-27.

[58] R.P. Kesner, G. Farnsworth and B.V. DiMattia, Double dissociation of egocentric and allocentric space following medial prefrontal and parietal cortex lesions in the rat, *Behav Neurosci*, 103 (1989) 956-961.

[59] E.A. Kharlamov, P.I. Jukkola, K.L. Schmitt and K.M. Kelly, Electrobehavioral characteristics of epileptic rats following photothrombotic brain infarction, *Epilepsy Res*, 56 (2003) 185-203.

[60] A.E. Kincaid and C.J. Wilson, Corticostriatal innervation of the patch and matrix in the rat neostriatum, *J Comp Neurol*, 374 (1996) 578-592.

[61] A.E. Kincaid, T. Zheng and C.J. Wilson, Connectivity and convergence of single corticostriatal axons, *J Neurosci*, 18 (1998) 4722-4731.

[62] V. King and J.V. Corwin, Neglect following unilateral ablation of the caudal but not the rostral portion of medial agranular cortex of the rat and the therapeutic effect of apomorphine, *Behav Brain Res*, 37 (1990) 169-184.

[63] V. King and J.V. Corwin, Spatial deficits and hemispheric asymmetries in the rat following unilateral and bilateral lesions of posterior parietal or medial agranular cortex, *Behav Brain Res*, 50 (1992) 53-68.

[64] V. King and J.V. Corwin, Comparisons of hemi-inattention produced by unilateral lesions of the posterior parietal cortex or medial agranular prefrontal cortex in rats: Neglect, extinction, and the role of stimulus distance, *Behav Brain Res*, 54 (1993) 117-131.

[65] V. King, J.V. Corwin and R.L. Reep, Production and characterization of neglect in rats with unilateral lesions of ventrolateral orbital cortex, *Exp Neurol*, 105 (1989) 287-99.

[66] H. Kita and S.T. Kitai, Glutamate-decarboxylase immunoreactive neurons in rat neostriatum - Their morphological types and populations, *Brain Res*, 447 (1988) 346-352.

[67] P. Landry, C.J. Wilson and S.T. Kitai, Morphological and electrophysiological characteristics of pyramidal tract neurons in the rat, *Exp Brain Res*, 57 (1984) 177-190.

[68] D. Lanens, M. Spanoghe, J. Vanaudekerke, A. Vanderlinden and R. Dommisse, complementary use of T2-weighted and postcontrast T1-weighted NMR images for the sequential monitoring of focal ischemic lesions in the rat-brain, *Magn Reson Imaging*, 11 (1993) 675-683.

[69] B. Lavoie and A. Parent, Immunohistochemical study of the serotoninergic innervation of the basal ganglia in the squirrel-monkey, *J Comp Neurol*, 299 (1990) 1-16.

[70] V.M. Lee, N.G. Burdett, T.A. Carpenter, L.D. Hall, P.S. Pambakian, S. Patel, N.I. Wood, M.F. James and B. Watson, Evolution of photochemically induced focal cerebral ischemia in the rat: Magnetic resonance imaging and histology, *Stroke*, 27 (1996) 2110-2119.

[71] M. Levesque, A. Charara, S. Gagnon, A. Parent and M. Deschenes, Corticostriatal projections from layer V cells in rat are collaterals of long-range corticofugal axons, *Brain Res*, 709 (1996) 311-315.

[72] M.O. Lopez-Figueroa, J.A. Ramirez-Gonzalez and I. Divac, Projections from the visual areas to the neostriatum in rats. A re-examination, *Acta Neurobiol Exp (Wars)*, 55 (1995) 165-175.

[73] J.W. Marshall, H.F. Baker and R.M. Ridley, Contralesional neglect in monkeys with small unilateral parietal cortical ablations, *Behav Brain Res*, 136 (2002) 257-65.

[74] N.R. McFarland and S.N. Haber, Convergent inputs from thalamic motor nuclei and frontal cortical areas to the dorsal striatum in the primate, *J Neurosci*, 20 (2000) 3798-813.

[75] A.J. McGeorge and R.L.M. Faull, The organization and collateralization of corticostriate neurons in the motor and sensory cortex of the rat-brain, *Brain Res*, 423 (1987) 318-324.

[76] A.J. McGeorge and R.L.M. Faull, The organization of the projection from the cerebral cortex to the striatum in the rat, *Neuroscience*, 29 (1989) 503-537.

[77] M.M. Mesulam, Large-scale neurocognitive networks and distributed processing for attention, language, and memory, *Ann Neurol*, 28 (1990) 597-613.

[78] K. Nakano, Neural circuits and topographic organization of the basal ganglia and related regions, *Brain Dev-Jpn* (2000) S5-S16.

[79] K. Nakano, T. Kayahara, T. Tsutsumi and H. Ushiro, Neural circuits and functional organization of the striatum, *J Neurol*, 247 (2000) 1-15.

[80] A. Nambu, K. Kaneda, H. Tokuno and M. Takada, Organization of corticostriatal motor inputs in monkey putamen, *J Neurophysiol*, 88 (2002) 1830-1842.

[81] J.A. Napieralski, A.K. Butler and M.F. Chesselet, Anatomical and functional evidence for lesion-specific sprouting of corticostriatal input in the adult rat, *J Comp Neurol*, 373 (1996) 484-97.

[82] E.J. Neafsey, E.L. Bold, G. Haas, K.M. Hurley-Gius, G. Quirk, C.F. Sievert and R.R. Terreberry, The organization of the rat motor cortex: A microstimulation mapping study, *Brain Res Rev*, 11 (1986) 77-96.

[83] S.P. Onn, A.R. West and A.A. Grace, Dopamine-mediated regulation of striatal neuronal and network interactions, *Trends Neurosci*, 23 (2000) S48-S56.

[84] A. Parent, Extrinsic Connections of the Basal Ganglia, *Trends Neurosci*, 13 (1990) 254-258.

[85] A. Parent and L.-N. Hazrati, Functional anatomy of the basal ganglia. I. The cortico-basal ganglia-thalamo-cortical loop, *Brain Res Rev*, 20 (1995) 91-127.

[86] A. Parent, F. Sato, Y. Wu, J. Gauthier, M. Levesque and M. Parent, Organization of the basal ganglia: the importance of axonal collateralization, *Trends Neurosci*, 23 (2000) S20-S27.

[87] G. Paxinos and C. Watson, *The Rat Brain in Stereotaxic Coordinates*, 2nd ed, Academic Press, Sydney, 1986.

[88] P.H. Pevsner, J.W. Eichenbaum, D.C. Miller, G. Pivawer, K.D. Eichenbaum, A. Stern, K.L. Zakian and J.A. Koutcher, A photothrombotic model of small early ischemic infarcts in the rat brain with histologic and MRI correlation, *J Pharmacol Toxicol Methods*, 45 (2001) 227-233.

[89] L. Prensa and A. Parent, The nigrostriatal pathway in the rat: A single-axon study of the relationship between dorsal and ventral tier nigral neurons and the striosome/matrix striatal compartments, *J Neurosci*, 21 (2001) 7247-7260.

[90] S. Ramón y Cajal, *Histology of the Nervous System of Man and Vertebrates*, Oxford University Press, New York, 1995.

[91] R.L. Reep, H.C. Chandler, V. King and J.V. Corwin, Rat posterior parietal cortex: Topography of corticocortical and thalamic connections, *Exp Brain Res*, 100 (1994) 67-84.

[92] R.L. Reep, J.L. Cheatwood and J.V. Corwin, The associative striatum: organization of cortical projections to the dorsocentral striatum in rats, *J Comp Neurol*, 467 (2003) 271-92.

[93] R.L. Reep and J.V. Corwin, Topographic organization of the striatal and thalamic connections of rat medial agranular cortex, *Brain Res*, 841 (1999) 43-52.

[94] R.L. Reep, J.V. Corwin, A. Hashimoto and R.T. Watson, Afferent connections of medial precentral cortex in the rat, *Neurosci Lett*, 44 (1984) 247-52.

[95] R.L. Reep, J.V. Corwin, A. Hashimoto and R.T. Watson, Efferent connections of the rostral portion of medial agranular cortex in rats, *Brain Res Bull*, 19 (1987) 203-21.

[96] R.L. Reep, J.V. Corwin and V. King, Neuronal connections of orbital cortex in rats: Topography of cortical and thalamic afferents, *Exp Brain Res*, 111 (1996) 215-32.

[97] R.L. Reep, G.S. Goodwin and J.V. Corwin, Topographic organization in the corticocortical connections of medial agranular cortex in rats, *J Comp Neurol*, 294 (1990) 262-80.

[98] A. Rosell and J.M. Gimenez-Amaya, Anatomical re-evaluation of the corticostriatal projections to the caudate nucleus: A retrograde labeling study in the cat, *Neurosci Res*, 34 (1999) 257-269.

[99] G.J. Royce, Laminar origin of cortical-neurons which project upon the caudate-nucleus - A horseradish-peroxidase investigation in the cat, *J Comp Neurol*, 205 (1982) 8-29.

[100] G.J. Royce, Cortical-neurons with collateral projections to both the caudate-nucleus and the centromedian-parafascicular thalamic complex - A fluorescent retrograde double labeling study in the cat, *Exp Brain Res*, 50 (1983) 157-165.

[101] F. Sato, P. Lavallee, M. Levesque and A. Parent, Single-axon tracing study of neurons of the external segment of the globus pallidus in primate, *J Comp Neurol*, 417 (2000) 17-31.

[102] N. Schmitzer-Torbert and A.D. Redish, Neuronal activity in the rodent dorsal striatum in sequential navigation: Separation of spatial and reward responses on the multiple T task, *J Neurophysiol*, 91 (2004) 2259-2272.

[103] M. Schroeter, S. Jander and G. Stoll, Non-invasive induction of focal cerebral ischemia in mice by photothrombosis of cortical microvessels: Characterization of inflammatory responses, *J Neurosci Methods*, 117 (2002) 43-49.

[104] L.D. Selemon and P.S. Goldman-Rakic, Longitudinal topography and interdigitation of corticostriatal projections in the rhesus monkey, *J Neurosci*, 5 (1985) 776-794.

[105] L.D. Selemon and P.S. Goldman-Rakic, Common cortical and subcortical targets of the dorsolateral prefrontal and posterior parietal cortices in the rhesus monkey: Evidence for a distributed neural network subserving spatially guided behavior, *J Neurosci*, 8 (1988) 4049-4068.

[106] Y. Smith, B.D. Bennett, J.P. Bolam, A. Parent and A.F. Sadikot, Synaptic relationships between dopaminergic afferents and cortical or thalamic input in the sensorimotor territory of the striatum in monkey, *J Comp Neurol*, 344 (1994) 1-19.

[107] Y. Smith and J.Z. Kieval, Anatomy of the dopamine system in the basal ganglia, *Trends Neurosci*, 23 (2000) S28-S33.

[108] P. Somogyi, J.P. Bolam and A.D. Smith, Mono-synaptic cortical input and local axon collaterals of identified striatonigral neurons - A light and electron-microscopic study using the golgi-peroxidase transport-degeneration procedure, *J Comp Neurol*, 195 (1981) 567-584.

[109] K. Sukekawa, Reciprocal connections between medial prefrontal cortex and lateral posterior nucleus in rats, *Brain Behav Evol*, 32 (1988) 246-251.

[110] F.G. Szele, C. Alexander and M.F. Chesselet, Expression of molecules associated with neuronal plasticity in the striatum after aspiration and thermocoagulatory lesions of the cerebral cortex in adult rats, *J Neurosci*, 15 (1995) 4429-48.

[111] M. Takada, H. Tokuno, A. Nambu and M. Inase, Corticostriatal projections from the somatic motor areas of the frontal cortex in the macaque monkey: segregation versus overlap of input zones from the primary motor cortex, the supplementary moter area, and the premotor cortex, *Exp Brain Res*, 120 (1998) 114-128.

[112] K. Uryu, L. MacKenzie and M.F. Chesselet, Ultrastructural evidence for differential axonal sprouting in the striatum after thermocoagulatory and aspiration lesions of the cerebral cortex in adult rats, *Neuroscience*, 105 (2001) 307-16.

[113] N. Van Bruggen, B. Cullen, M. King, M. Doran, S. Williams, D. Gadian and J. Cremer, T2- and diffusion-weighted magnetic resonance imaging of a focal ischemic lesion in rat brain, *Stroke*, 23 (1992) 576-582.

[114] G.W. Van Hoesen, E.H. Yeterian and R. Lavizzo-Mourey, Widespread corticostriate projections from temporal cortex of the rhesus monkey, *J Comp Neurol*, 199 (1981) 205-19.

[115] T.M. Van Vleet, K.J. Burcham, J.V. Corwin and R.L. Reep, Unilateral destruction of the medial agranular cortical projection zone in the dorsocentral striatum produces severe neglect in rats, *Psychobiology*, 28 (2000) 57-66.

[116] T.M. Van Vleet, S.A. Heldt, J.V. Corwin and R.L. Reep, Infusion of apomorphine into the dorsocentral striatum produces acute drug-induced recovery from neglect produced by unilateral medial agranular cortex lesions in rats, *Behav Brain Res*, 143 (2003) 147-57.

[117] T.M. Van Vleet, S.A. Heldt, K.R. Guerrettaz, J.V. Corwin and R.L. Reep, Unilateral destruction of the dorsocentral striatum in rats produces neglect but not extinction to bilateral simultaneous stimulation, *Behav Brain Res*, 136 (2002) 375-87.

[118] T.M. Van Vleet, S.A. Heldt, B. Pyter, J.V. Corwin and R.L. Reep, Effects of light deprivation on recovery from neglect and extinction induced by unilateral lesions of the medial agranular cortex and dorsocentral striatum, *Behav Brain Res*, 138 (2003) 165-78.

[119] J.M. Vargo, J.V. Corwin, V. King and R.L. Reep, Hemispheric asymmetry in neglect produced by unilateral lesions of dorsomedial prefrontal cortex in rats, *Exp Neurol*, 102 (1988) 199-209.

[120] J.M. Vargo and J.F. Marshall, Time-dependent changes in dopamine agonist-induced striatal Fos immunoreactivity are related to sensory neglect and its recovery after unilateral prefrontal cortex injury, *Synapse*, 20 (1995) 305-315.

[121] J.M. Vargo and J.F. Marshall, Frontal cortex ablation reversibly decreases striatal zif/268 and junB expression: temporal correspondence with sensory neglect and its spontaneous recovery, *Synapse*, 22 (1996) 291-303.

[122] J.M. Vargo and J.F. Marshall, Unilateral frontal cortex ablation producing neglect causes time-dependent changes in striatal glutamate receptors, *Behav Brain Res*, 77 (1996) 189-199.

[123] J. Verlooy, J. Vanreempts, G. Peersman, F. Vandevyver, B. Vandeuren, M. Borgers and P. Selosse, Photochemically-induced cerebral infarction in the rat - Comparison of NMR imaging and histologic-changes, *Acta Neurochir (Wien)*, 122 (1993) 250-256.

[124] J.R. Walters, D.N. Ruskin, K.A. Allers and D.A. Bergstrom, Pre- and postsynaptic aspects of dopamine-mediated transmission, *Trends Neurosci*, 23 (2000) S41-S47.

[125] B.D. Watson, Animal Models of Photochemically Induced Brain Ischemia and Stroke. In M.D. Ginsberg and J. Bogousslavsky (Eds.), *Cerebrovascular Disease: Pathophysiology, Diagnosis, and Management*, Blackwell Science, Malden, Mass., USA, 1998, pp. 52-73.

[126] B.D. Watson, W.D. Dietrich, R. Busto and M.D. Ginsberg, Photochemically induced thrombotic stroke in rat-brain, *Ann Neurol*, 14 (1983) 126-126.

[127] B.D. Watson, W.D. Dietrich, R. Busto, M.S. Wachtel and M.D. Ginsberg, Induction of Reproducible Brain Infarction by Photochemically Initiated Thrombosis, *Ann Neurol*, 17 (1985) 497-504.

[128] B.D. Watson, W.D. Dietrich, R. Prado and M.D. Ginsberg, Argon laser-induced arterial photothrombosis. Characterization and possible application to therapy of arteriovenous malformations, *J Neurosurg*, 66 (1987) 748-54.

[129] C. Wiessner, F.M. Bareyre, P.R. Allegrini, A.K. Mir, S. Frentzel, M. Zurini, L. Schnell, T. Oertle and M.E. Schwab, Anti-Nogo-A antibody infusion 24 hours after experimental stroke improved behavioral outcome and corticospinal plasticity in normotensive and spontaneously hypertensive rats, *J Cereb Blood Flow Metab*, 23 (2003) 154-65.

[130] C.J. Wilson, Postsynaptic potentials evoked in spiny neostriatal projection neurons by stimulation of ipsilateral and contralateral neocortex, *Brain Res*, 367 (1986) 201-13.

[131] C.J. Wilson, Morphology and synaptic connections of crossed corticostriatal neurons in the rat, *J Comp Neurol*, 263 (1987) 567-580.

[132] C.J. Wilson, The generation of natural firing patterns in neostriatal neurons, *Prog Brain Res*, 99 (1993) 277-97.

[133] C.J. Wilson, Basal ganglia. In G. Shepherd (Ed.), *The Synaptic Organization of the Brain*, Oxford University Press, NY, 1998.

[134] A.K. Wright, L. Norrie, C.A. Ingham, E.A. Hutton and G.W. Arbuthnott, Double anterograde tracing of outputs from adjacent "barrel columns" of rat somatosensory cortex. Neostriatal projection patterns and terminal ultrastructure, *Neuroscience*, 88 (1999) 119-33.

[135] Y. Wu, S. Richard and A. Parent, The organization of the striatal output system: A single-cell juxtacellular labeling study in the rat, *Neurosci Res*, 38 (2000) 49-62.

[136] E.H. Yeterian and G.W. Van Hoesen, Cortico-striate projections in the rhesus monkey: The organization of certain cortico-caudate connections, *Brain Res*, 139 (1978) 43-63.

[137] K. Zilles and A. Wree, The rat nervous system: Forebrain and midbrain. In G. Paxinos (Ed.), *The Rat Nervous System*, Academic Press, Sydney, 1985, pp. 375-415.

BIOGRAPHICAL SKETCH

Joseph Laton Cheatwood was born and raised in rural Polk County, Florida. He graduated from Lake Gibson High School in 1994. He received a BS in biology from Stetson University (DeLand, Florida) on May 10, 1998. On May 11, 1998, he began graduate school at the University of Florida, completing his MS in Veterinary Medical Sciences in December, 2000. Immediately thereafter, Joseph joined the lab of Roger Reep, PhD, and began his studies in the neurosciences. After completion of his PhD in August 2004, Joseph will begin a postdoctoral fellowship at Loyola University, Chicago.